1970

Design and construction of a system for measurement of unsteady propeller forces.

Horton, Charles O.

Massachusetts Institute of Technology

DESIGN AND CONSTRUCTION OF A SYSTEM FOR MEASUREMENT OF UNSTEADY PROPELLER FORCES

Charles O. Horton

DESIGN AND CONSTRUCTION OF A SYSTEM FOR MEASUREMENT OF UNSTEADY PROPELLER FORCES

by

Charles O. Horton

B.S., University of Louisville

(1962)

SUBMITTED IN PARTIAL FULFILLMENT

OF THE REQUIREMENTS FOR THE

DEGREE OF NAVAL ENGINEER

AND MASTER OF SCIENCE

at the

MASSACHUSETTS INSTITUTE OF

TECHNOLOGY

June, 1970

TABLE OF CONTENTS

TABLE OF CONTENTS

TABLE OF CONTENTS

ACKNOWLEDGEMENTS

It is standard practice in most papers to give credit to individuals who have been helpful to the author. Because of the breadth of coverage of this thesis and the circumstances from which the topic arose, this is especially true in this case.

My thesis supervisor, Dr. Justin E. Kerwin and Assistant Professor Damon E. Cummings were the originators of the proposal which eventually led to the thesis. They have both been patient and understanding in providing help, advice and background information.

Personnel of the MIT IL-7, coordinated by George Suntheimer, delivered ideas, drawings and hardware in timely fashion. They were always cooperative and enthusiastic.

Lastly, I wish to thank Dean Lewis, the engineer in charge of the propeller tunnel and chief advisor in questions relating to practical mechanical engineering. Dean also kept track of purchase orders and in general was a one man supply department.

LIST OF FIGURES

I - INTRODUCTION

In 1968, a proposal was made to the National Science Foundation that the MIT Department of Naval Architecture and Marine Engineering undertake a program of experimental study of unsteady hydrodynamic forces [1]. The proposal to the NSF advocated modification of MIT's variable pressure water tunnel to permit measurement of propeller generated forces in six degrees of freedom. The proposal recommended the design and acquisition of a dynamic pressure transducer and purchase of signal processing and analysis equipment for both shaft and pressure measurements. The NSF grant in response to this proposal provided funding for a two year program of investigation and equipment acquisition.

Dr. Justin E. Kerwin was the project supervisor and Dr. Damon E. Cummings was a participating faculty member. Dr. Reinder Wereldsma, on a one year visit to the USA from the Netherlands Ship Model Basin, was also a participating faculty member.

Work on this project was undertaken by this investigator as a thesis topic late in the fall term of 1969. The primary goal of this thesis is to provide an operating six degree of freedom propeller force measuring system. This goal is in partial fulfillment of the NSF grant. In meeting this immediate goal, consideration has been given to the further goal of installing pressure measuring devices and incorporating them into the overall program of investigation.

Unlike most master's theses which treat a single well-defined subject in detail, this thesis treats a single project in as much breadth in scope and depth of detail in specialized subject areas as is possible in a semester's work. The effort is an attempt to explore the requirements dictated by several academic and engineering disciplines and to successfully integrate these requirements in completing the project.

One of the author's goals in the writing of this thesis is to assemble all that he has learned about the project and to explain it so that successors on the project can use this thesis as documentation in performing their own work. Thus this thesis can serve as a single reference to answer questions concerning system construction and operation. This will permit other students to devote most of their time to furthering their special projects.

II - THE M.I.T. PROPELLER TUNNEL

The MIT propeller tunnel was built in 1938-39 and provided a significant advance in propeller test facilities at that time [2]. Since then, several modifications have been made to the tunnel to extend its useful life, to make it more convenient to use, and to give it additional capabilities in keeping with current research needs.

General Features.

The tunnel is a closed return type and is approximately a 24 foot diameter square in shape. See figure I-1. It occupies parts of the first and second floors of Building 3 on the MIT campus. The smallest internal diameter is approximately 30 inches, but this gradually widens to a 60 inch maximum before narrowing again to enter the test section. The tunnel cross section is circular except at the test section and in the tapered transition section. The transition section narrows the 60 inch circular cross section to the 20 inch square test section.

Testing Facilities.

The tunnel can provide water velocities in the test section up to 33 ft/sec and maintain any selected internal pressure from atmospheric (760 mm Hg) down to approximately 140 mm Hg.

The present propeller testing installation is normally operated in the range of 500-2000 RPM. Measurements can be taken on thrust up to 500 lbs and torque up to 500 in-lbs on 12 inch or smaller diameter propellers. These thrust and torque readings are accurate to $\pm \frac{1}{2}$ lb and $\pm \frac{1}{2}$ in-lb respec-

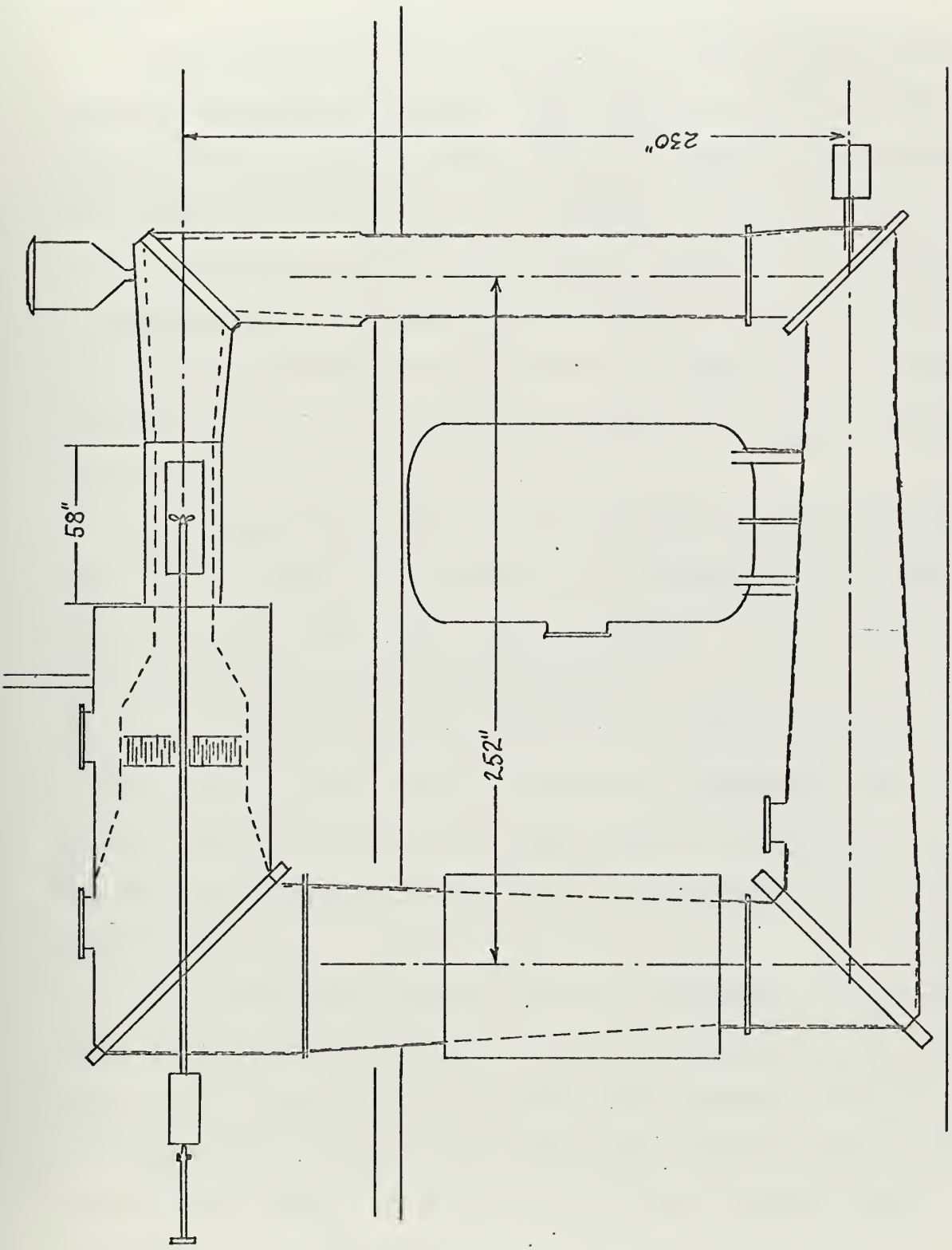

FIGURE II-1

tively. The two degree of freedom system uses a custom made Lebow dynamometer which has strain gage bridges for sensing elements.

The test section is accessible via any of four identical removable plexiglass windows. The windows are 2.0 inches thick by $44^{7}/_{16}$ in. long and $15^{5}/_{16}$ in. high and cover access holes measuring $13^{7}/_{16}$ by $41^{15}/_{16}$ inches. They are readily cut or drilled and are thus ideal for mounting experiments. One apparatus allows measuring six degree of freedom forces on lifting surfaces, such as rudders or hydrofoils. Fittings are installed in the windows to accept Pitot tubes at several locations.

The tunnel may also be operated with a free surface to test surface piercing hydrofoils or to simulate a miniature towing tank for small ship model testing.

Propeller and Impeller Drive Systems.

Most of the original equipment is still in use to provide tunnel water flow and drive the propeller test shaft. Some refinements have been added, but otherwise the original components have given satisfactory service for over 30 years.

A 100 HP motor drives three DC generators. One of these, a 60 KW shunt wound generator, provides power for the 75 HP DC impeller drive motor. The second, a 30 KW shunt wound DC generator, provides power for the 40 HP propeller drive motor. The third is a 3 KW compound wound DC generator and provides excitation for both large DC

generators.

A variable resistance vernier control system provides close control of both impeller and propeller RPM. A 60 tooth gear mounted on the drive shaft immediately forward of the torque measuring device is used in conjunction with a magnetic pickup (also of Lebow manufacture) to provide a 60 pulse per revolution signal.

A similar device attached to the impeller drive shaft also provides a 60 pulse per revolution output. Either signal may be fed to a Hewlett-Packard 5212A electronic counter. By using 60 pulses per revolution, the counter reads directly in RPM instead of RPS.

Propeller Drive Shaft and Housing.

The propeller drive shaft is a continuous length of stainless steel tubing which is supported at numerous points by teflon coated bronze bearings. The tubing has a 16 microinch finish obtained by a centerless grinding process to provide a very smooth surface to ride in the teflon bearings. This prolongs the bearing and shaft life and reduces the power needed to drive the shaft. Lubrication of the bearings is by water retained in the shaft housing. The shaft housing is made from stainless steel pipe sections joined by stainless steel couplings which also serve as bearing housings. The shaft housing consists of three 36 inch long sections and three 18 inch long sections.

The propeller end of the drive shaft is enclosed and supported by a cast bronze housing. The taper from the

3.975 inch O.D. to the 2.375 inch final O.D. is derived from a cosine function. The taper runs a distance of approximately 35 inches in the overall length of 39 inches of the housing section. It provides a very satisfactory inlet flow to the model propellers.

Because the tunnel is used for many different purposes, many of which do not employ the propeller testing shaft, it is necessary to be able to retract the shaft from the test section. It is desirable to accomplish the retraction without draining the tunnel each time, completely removing the shaft, and sealing the hole. This means that the shaft housing must have a seal at the drive end and the housing must have its own water supply for bearing lubrication.

To allow easy passage of the shaft housing through the tunnel wall and through the honeycomb, the outer diameter of the pipe has been turned down .020 inches below the nominal 4.0 inch O.D. to make the outer surface smooth. Standard pipe comes with a rough finish. Water lubrication for the drive shaft bearings is provided by tap water kept in the assembled housing. Since all drive shaft components are of stainless steel or bronze, no special corrosion treatment is necessary. However, a small water pressure is kept on the housing to make up for loss of lubricating water when the tunnel is drained between experiments. This is done because loss of water from the housing could not be detected and running the shaft without water lubrication would have a disastrous effect on both the bearings and the

drive shaft. Small holes are drilled in the stainless steel shaft housing connecters to permit passage of lubricating water through the couplings.

Water Flow.

The original four-bladed bronze impeller is still used to provide water flow. It is located in the lower level horizontal run in the 30 inch diameter dection. It is immediately followed by straightening vanes to remove rotation from the water.

Each 90° bend has several thin stainless steel turning vanes with a non-symmetrical cross section developed from airfoil theory. The vanes have a low power loss and the resulting turbulence generated by rounding the corners is fine patterned and on the order of the turning vane spacing [3].

The 30 inch diameter widens out to 60 inches to slow the water velocity and further reduce turbulence. The effect sought is similar to a stream dumping into a reservoir. After rounding a 90° bend the water is passed through a honeycomb of one inch diameter plastic tubes.

The 60 inch diameter is then smoothly constricted to flow through the 20 inch square test section. The section area reduction is 7.07. The constriction speeds up the flow velocity and at the same time stretches out any remaining turbulence. A quite smooth flow pattern results.

The Variable Pressure System.

Any pressure in the range of atmospheric to 140 mm can be maintained by the vacuum pump. The lower limit is

dictated by the vapor pressure of water and small air leaks in the tunnel. Water vapor pressure at 60°F is 135 mm Hg.

Suction from the vacuum pump is taken at three points on the tunnel: (1) from the vacuum dome, (2) from the manhole cover over the 60" horizontal section and (3) at the last 90° bend before entering the honeycomb.

If the tunnel is completely filled with water, some water may be sucked into the vacuum line to the pump. This is trapped in a receiver tank. Suction by the pump is taken from the top of the tank, while a drain line is provided at the bottom of the tank. The drain line drops 35 feet and is kept below water in the building basement. No matter how good the tunnel vacuum, the water cannot be lifted 35 feet to the separation tank, nor can air enter the system because of the water seal.

The vacuum system is the primary means of removing dissolved gases from the tunnel water. Dissolved oxygen is chemically removed for corrosion protection of the mild steel walls, and other gases are removed by keeping the tunnel at reduced pressure for several hours. If this is not done, dissolved gases form bubbles at reduced pressures and obscure the viewing of experiments in the test section.

The Drain Tank.

The tunnel has a water storage tank of 1,380 gallon (approximately 184.2 ft^3) capacity. This volume is sufficient to hold the water drained from the tunnel in order to lower the water level below the floor of the test section. Water drained to the storage tank can be pumped back into the tunnel in about five minutes.

The storage tank is both a convenience and a necessity. Because some water can be removed from the tunnel and stored at ambient temperature conditions, the water temperature remains virtually constant in the tunnel, even over a series of drain and refill cycles. This permits continuation of an experiment at the same water temperature, or avoids the need to make temperature corrections in the results.

In the course of setting up a new experiment and running it, it may be necessary to drain down the tunnel to get access to the test section, refill the tunnel and make another trial run several times. Having the drain tank allows reusing the same water over and over. This factor alone saves time, since refilling the tunnel from the city water main requires nearly an hour.

By using the same water repeatedly, it is necessary to treat it with sodium nitrite only occasionally to remove dissolved oxygen. If fresh water were frequently added to the tunnel as make-up after partially draining down the system, large amounts of sodium nitrite would be used annually at a considerable cost in both dollars and man-

hours.

Tunnel water must be deaerated, filtered to maintain visibility in the test section and treated to inhibit corrosion; therefore, much time can be saved by reusing it. Such treatment is essential if good visibility is to be maintained in the test section, because dissolved gases readily form bubbles when the tunnel is operated at reduced pressures.

Though some air is dissolved in the water which is cycled through the tank each time the tunnel is partially drained and refilled, this amount of air (and oxygen) should be much less than that which would be introduced by refilling from the city water main. Since the only water surfaces exposed to air are in the storage tank and the tunnel, and the process does not involve much stirring of the water, aeration is minimized.

Addition of fully aerated water to the tunnel in the amount equal to the drain tank volume could potentially add as much as 4.5 ft^3 of dissolved air to the system. If treated tunnel water is caused to reach only 10-20 percent saturation by draining to the tank and refilling, only .45 to .90 ft^3 of air is introduced.

III - THE UNSTEADY PROPELLER FORCE MEASURING SYSTEM

Generation of Propeller Forces.

Circumferential variations in the velocity field in which a propeller operates cause periodic variations in the lift and drag of each blade. The lift and drag variations on each blade generate periodic forces and moments which act on the propeller shaft and bearings. These changes in blade output also create changes in the pressure field surrounding the blade, but these pressure changes will not be discussed in this report.

The fundamental frequency of these force and moment variations is known as the blade frequency and is given by

$$f_1 = \text{RPM} \times N$$

where N is the number of blades on the propeller and f_1 is the first harmonic. The character of the wake and the details of construction of a propeller may generate forces of a higher frequency. Such forces will generally occur at frequencies which are integral multiples of blade frequency.

Vibrations of individual blades will not in general be harmonics of blade frequency. Blade vibrations depend upon the geometry of the blade and are independent of the flow velocity field and the RPM.

Calling the blade frequency the fundamental implicitly assumes:

1. each blade of a propeller is identical

2. at the same θ, each blade will produce the same shaft and bearing forces and moments

The second assumption implies yet a third assumption:

3. the flow condition in which the propeller is operating does not change with time.

These conditions are definitely not met in the full scale ship propeller, but they can be closely approximated by a model propeller in a testing tunnel or tow tank.

Although other types of tests not involving these assumptions can probably be performed by the six degree of freedom sensor, these are the central assumptions in the development of the data collection and analysis system. See figure III-1 for the estimated shape and magnitude of these forces.

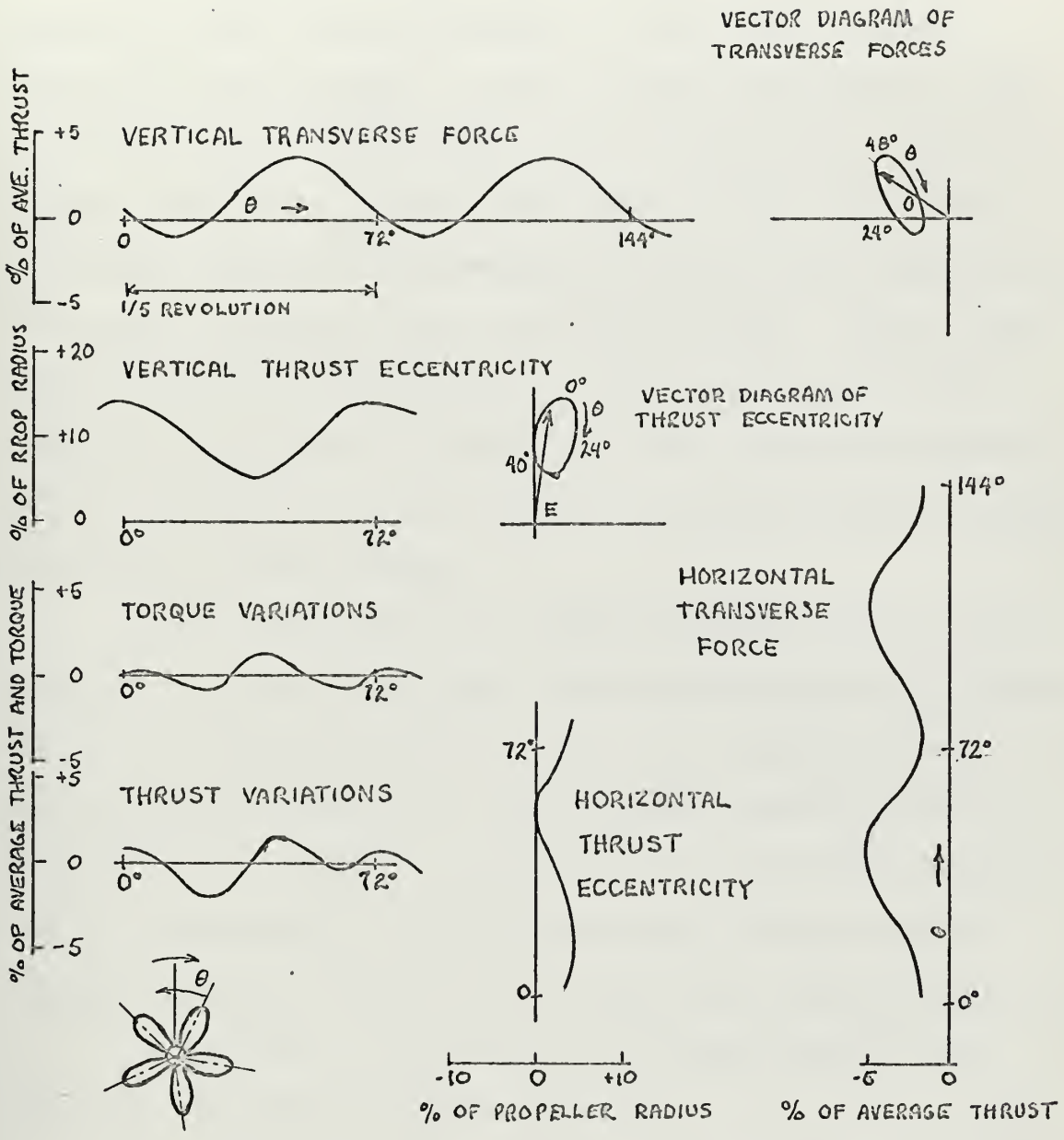

DYNAMIC PHENOMENA OCCURRING ON A FIVE-BLADED PROPELLER IN OPERATIONAL CONDITION [4]

FIGURE III-1

Six Degree of Freedom Sensors.

Six degree of freedom sensors have only become possible since the development of very small, highly sensitive strain gages. Prior to this development, only propeller thrust and torque could be measured. At first, purely mechanical systems were used. These were called balances because of the systems of levers and weights that were used to measure the forces and torques. Next, dynamometers were developed which could measure thrust and torque. The latest of these use strain gages similar to those employed in the six degree of freedom sensor discussed as a part of this thesis.

In the last few years, NSRDC Carderock [5] and the Netherlands Ship Model Basin [6] have developed six degree of freedom measuring systems for model propeller tests. The MIT system parallels both of these installations in principle, but differs significantly in execution because of the constraints of differing tunnel designs and the special operating needs of the respective institutions.

In general, a six degree of freedom system must have the following characteristics:

a. high signal to noise ratio output from strain gages.

b. no natural frequencies in the band of operational frequency interest. It is highly desirable that there be no natural frequencies near the band of operational frequency interest.

c. efficient data collection and analysis system.

d. a precise timing pulse to mark the start of each shaft revolution to serve as a reference for measurement of forces and moments.

In addition, the following are highly desirable features:

a. system must interface with the existing tunnel design without causing undue compromise in either the six degree of freedom system or the existing tunnel operating features.

b. must of course cost less than or equal to the available funding to design and construct.

c. must be reasonably simple to assemble, operate and disassemble, in order to permit use of the tunnel for other experiments.

These mandatory and desirable characteristics involve conflicts and require that trade offs be made. A discussion of these trade offs follows.

Signal to Noise Ratio One approach to getting a high signal to noise ratio is to use a strain gage mounting with a low spring constant in each of the three directions of deflection so that low order forces will cause relatively large deflections of the gages. This approach is not feasible, since high shaft "k's" are required to keep shaft natural frequencies outside of the operating range. Thus a stiff shaft must be accepted, even though this means that strain gage deflection and outputs will be low.

The development of signal averaging has made possible

the recovery of signals which are below noise level [7]. The process involves digitizing the signal at regular intervals and storing the result in a digital memory. The process is initiated by a timing pulse which is repeated once each shaft revolution. In order for the signal averaging to give accurate results, the timing pulse must be repeated exactly at the same θ each revolution and the shaft RPM must be constant for the duration of the data collection period.

Because of the necessity for a stiff shaft, a combination of high amplification of strain gage outputs and signal averaging are the approaches taken to getting a high signal to noise ratio.

System Natural Frequencies.

All moving mechanical systems have natural frequencies. At a natural frequency the amplitude of deflection is limited only by the amount of damping in the system which acts to dissipate energy in that mode of vibration.

In the case of the propeller shafting system, there are three possible modes of vibration - torsion, bending and compression. The same basic equation describes all three modes, but the constants involved are different. In all modes of vibration, the shaft has more than a single degree of freedom, but for describing the modes and their effects, a single degree of freedom model is sufficient. A more detailed analysis is contained in the appendix. The single degree of freedom differential equation is:

$$M\ddot{z} + C\dot{z} + Kz = F_o \sin \omega t$$

where z = displacement

M = mass or inertia

C = damping constant

K = spring constant

F_o = maximum amplitude of driving force or moment

ω = frequency of driving force or moment

The solution to the single degree of freedom equation results in the relationship below which determines the system natural frequency. (This is the same for driven or free vibrations.)

$$\omega_n = \sqrt{K/M - (C/2M)^2}$$

If system damping is small, the second term under the radical is negligible and the expression for natural frequency is

$$\omega_n = \sqrt{K/M}$$

If the single degree of freedom model is retained for simplicity, the same discussion of vibrations will serve to describe conditions for all three modes. It should be noted that the torsional natural frequencies will not be the same as the compression mode natural frequencies, nor the bending mode. The degrees of freedom also may not be the same in all three modes.

The diagram below, figure III-2, illustrates the behavior of a single degree of freedom system. Note that the presence of system damping reduces the response amplitude as resonance is approached.

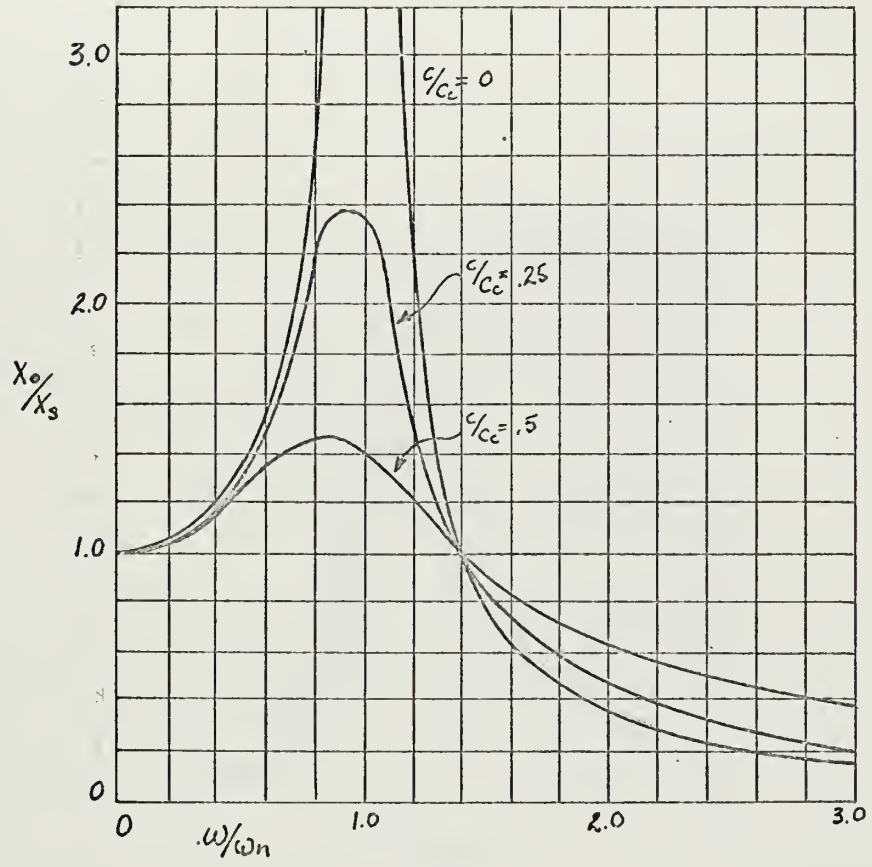

FIGURE III -2

In a dynamic force measuring system, the behavior of the phase angle between the applied force and the system response also becomes an important factor. As shown in figure III-2, a large amount of system damping causes the phase angle to change rapidly as a resonant frequency is approached. With no system damping, the phase angle stays at 0° until resonance at which time it flips to 180°.

A knowledge of phase angle behavior is vital to achieving accurate results. A minimum amount of system damping is desired in order that the phase angle remain at or near zero.

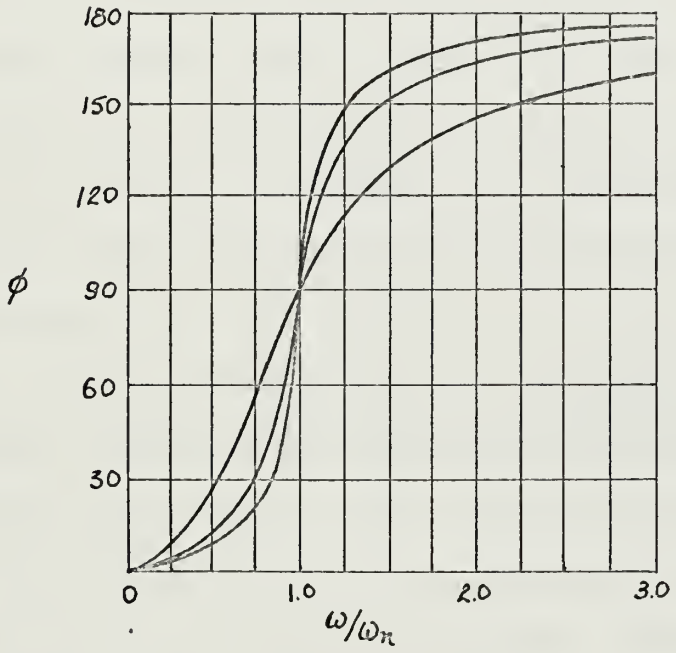

FIGURE III -3

Thus damping has a favorable effect on vibration amplitudes, but an unfavorable effect on the phase angle behavior.

The Measuring Unit and Shaft.

The measuring unit shaft is machined from type 303 stainless steel and has a maximum diameter of 2.07 inches, and a length overall (not including mating taper) of 12.25 inches. One end is tapered to accept NSRDC model propellers and the other is tapered to mate with the flywheel.

The strain gage bridges are located immediately upstream of the propeller mounting taper and the leads are fed through a hollow shaft to the solid state amplifiers. The six amplifiers are located in a centerline section which is .875 inches in diameter and approximately 3.25 inches long. They are potted for physical protection and waterproofing.

The reference timing pulse is supplied by a Foto-fet assembly mounted on the measuring unit shaft. The neon bulb and photosensor rotate with the shaft while the timing slit is held fixed by ball bearings which ride in slots machined in the flywheel housing. The ball bearings permit movement of the entire shaft assembly fore and aft by a little more than $\frac{1}{4}$ inch but keep the assembly rigid in the direction of rotation.

It was necessary to make the rotor and stator into a single assembly to maintain a close tolerance clearance between them. A small and very constant separation between the bulb, slit and photocell is required to provide a pulse with a constant amplitude and a period coinciding exactly

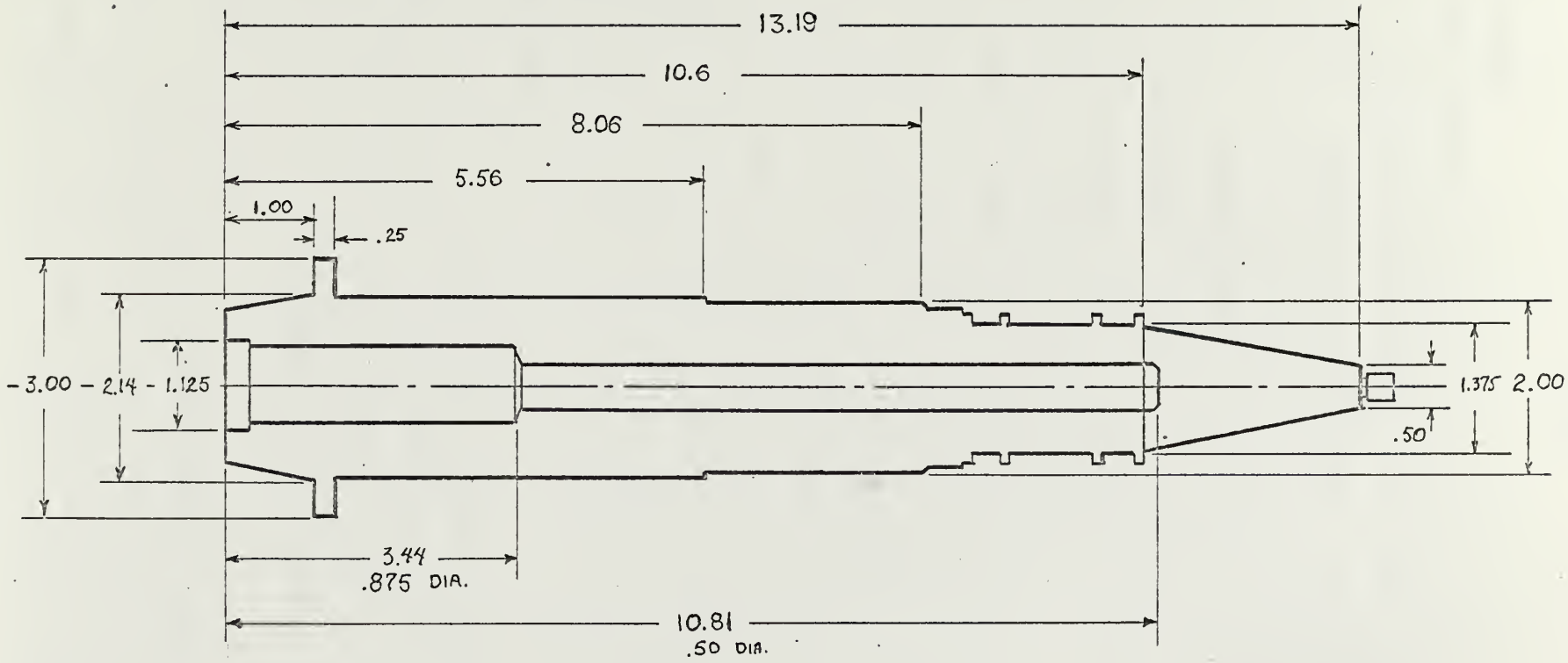

THE MEASURING UNIT AND SHAFT

FIGURE III-4

with the shaft revolution period.

The Flywheel.

The flywheel is machined from type 303 stainless steel. It has an outer diameter of $3.400 \pm .005$ inches and an inner diameter of 1.45 inches. At each end there is a tapered bore to provide an exact centering and alignment with the drive shaft and measuring unit shaft.

The approximate weight of the flywheel is 27.5 pounds. The size and material give a rotational inertia of 0.0842 slug-in^2 and a bending inertia of 0.0421.

A special thin walled tubing was used for the flywheel housing to allow the flywheel to have the maximum possible outer diameter. The housing wall thickness is only .188 inches to allow a clearance of .112 inches between the flywheel and the inner wall of the housing. A much higher flywheel inertia would be desirable in order to isolate the sensor as much as possible from external sources of vibration, but to do so would have required a choice between:

a. a larger shaft housing diameter and the necessary enlargement of the insertion hole in the tunnel wall and the support hole in the honeycomb. These modifications are not compatible with the present two degree of freedom system.

b. A larger shaft housing near the end of the shaft, but retention of four inch O.D. for the drive shaft housing. This would perhaps create a hydrodynamic

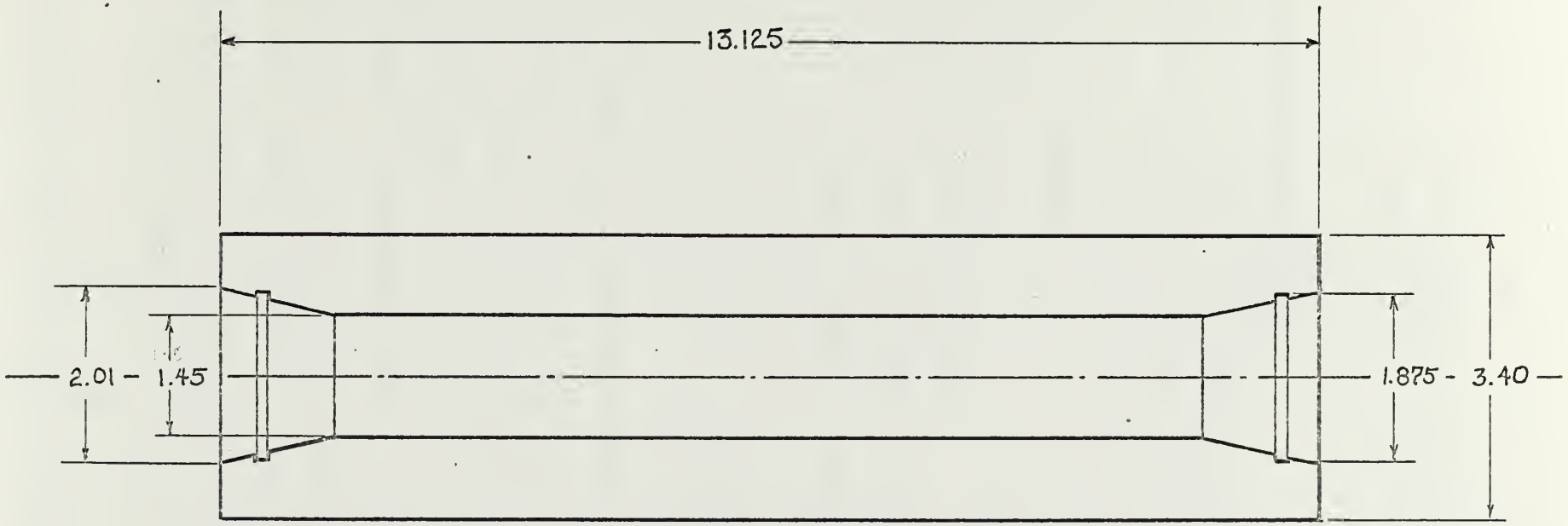

FLYWHEEL

FIGURE III-5

SEE DRAWING
IL-166894
FOR DETAILS

problem in the inlet flow to the propeller and would make the assembly of the flywheel and tailshaft a complex and difficult task, since assembly would have to be done within the test section.

The Drive Shaft and Housing.

The drive shaft is a single piece of stainless steel tubing approximately 172 inches long. The outer diameter is 1.75 inches and has been given a 16 microinch finish by a centerless grinding process. This surface finish provides a smooth bearing surface for long bearing and shaft life as well as smooth operation.

A special effort was made to procure a tubing section that was at or slightly over the manufacturer's specification for maximum diameter so that the shaft would be properly sized after the finish treatment. It is necessary to surface polish the entire shaft length so that any portion may be used as a bearing surface. This eases assembly because some of the bearings must be slid over the shaft for a distance of up to one-half of the shaft length. Also, in case an area intended for a bearing is undersized, the shaft can be exchanged end for end and the undersized area located to a new position in between the bearings. A slightly over length section of tubing was purchased to aid in making adjustments of this sort, since the shaft can be custom fitted by cutting a little off of one end or the other.

Stainless steel pipe with a surface finish or tubing

A FRONT HOUSING
B MEASURING UNIT SHAFT
C INTERMEDIATE HOUSING
D FLYWHEEL
E FLYWHEEL HOUSING
F FLOATING BEARING ASS'Y
G PROP. SHAFT ADAPTER
H PROP. DRIVE SHAFT
I SHAFT HOUSING
J HOUSING COUPLING

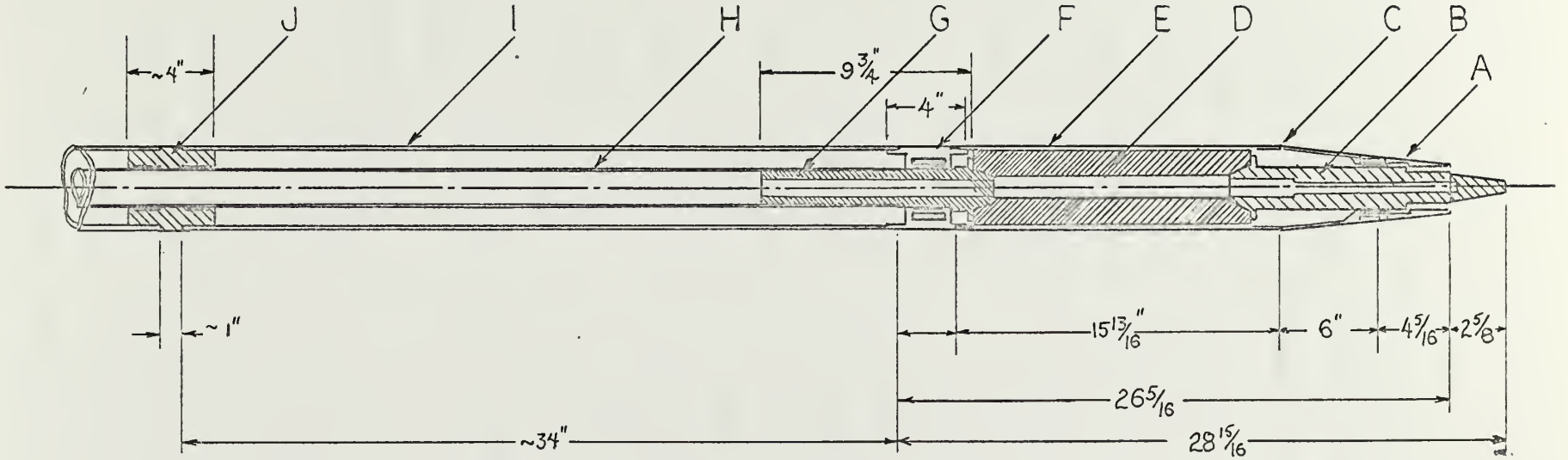

MEASURING UNIT AND SHAFT ASSEMBLY

FIGURE III-6

with a smooth surface will be used for the shaft housing. The joining sections will be machined from brass or bronze instead of stainless steel. Stainless steel on stainless steel tends to gall and makes assembly and disassembly very difficult. Stainless steel on brass makes a very satisfactory threaded joint.

The bearings used in the six degree of freedom shaft are of teflon coated mild steel rather than bronze as before. The bronze was preferred but could not be procured in the small quantity required. This means that instead of using tap water for lubrication, the water in the shaft housing must also be treated with sodium nitrite.

The shaft could be made free flooding with the tunnel except that the section forward of the flywheel which contains the Fotofet must be kept dry. A lubrication scheme similar to that used with the two degree of freedom shaft should suffice. See figure III-6

As in the two degree of freedom shaft housing, holes are drilled through the couplings to permit filling the housing with water.

Torsional Vibration Mode.

Torsion mode excitation is by fluctuation in propeller torque. Such fluctuation is normally at blade frequency at harmonics of blade frequency. The measuring unit shaft is made very stiff in torsion in order to keep the shaft torsion mode natural frequency well above the blade frequency and low order harmonics of blade frequency.

The purpose of the flywheel is to supply a vibration reference, or "ground" to the propeller and the sensor. An infinitely large flywheel would successfully isolate the sensor from torsional excitation originating upstream from the sensor. A very large flywheel inertia requires a very stiff shaft to have an acceptable natural frequency.

If the flywheel inertia is large with respect to propeller inertia and is torsionally isolated from other exciting forces, a model like the one in figure III-7 is applicable.

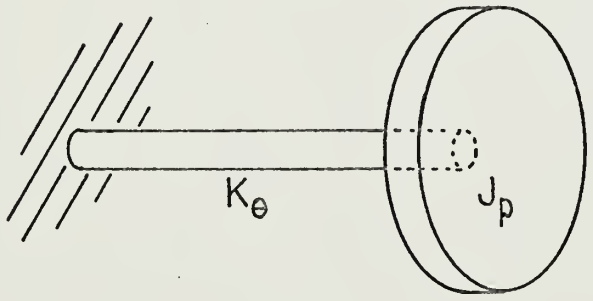

K_θ = SHAFT TORSIONAL STIFFNESS

J_p = PROPELLER INERTIA

$$\omega_n = \sqrt{K_\theta / J}$$

FIGURE III -7

The decision was made to keep the flywheel diameter small enough to fit within a 4 inch diameter housing to permit the entire shaft system to be interchangable with the present two-degree of freedom shaft system. This decision limited the maximum possible flywheel diameter and inertia. Thus the propeller inertia is no longer neglible in comparison to the flywheel inertia.

Now a model shown in figure III-8 must be considered.

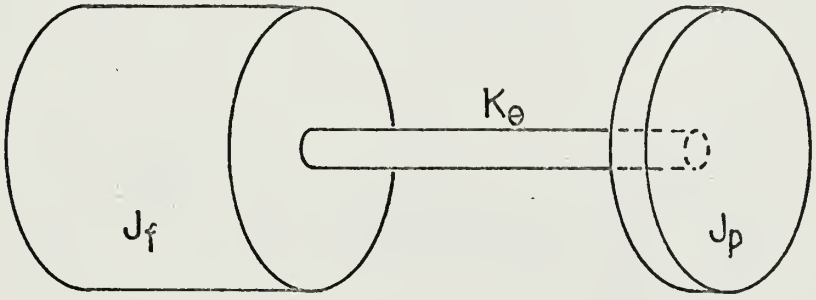

J_f = FLYWHEEL INERTIA

$$\omega_n = \sqrt{\frac{K_\theta (J_f + J_p)}{J_f \cdot J_p}}$$

FIGURE III -8

See appendix C for estimated torsional natural frequencies with various propeller inertias.

Compressional Vibration Mode.

As in the torsional case, the purpose of the flywheel is to isolate the sensor from the rest of the system. The difference between the propeller mass and the flywheel mass is much greater than the difference in rotational inertias (for 10 or 12 inch bronze propellers), so it follows that the flywheel should isolate compressive vibrations much more effectively than torsional vibrations.

The same equation and a similar model can be used to describe the sensor-flywheel compression mode behavior.

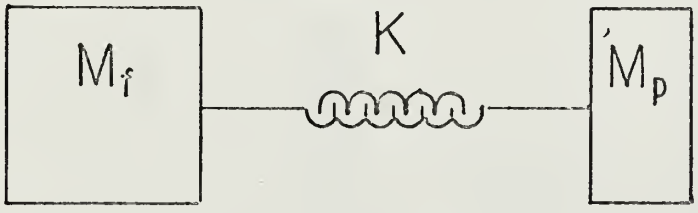

$$\omega_n = \sqrt{\frac{K\,(M_f + M_p)}{M_f \cdot M_p}}$$

FIGURE III-9

The compressional mode and the torsional mode are not independent. According to Lewis [8].

> The longitudinal and torsional motions of a propeller-shaft system are coupled by water inertia and damping. Provided the longitudinal frequency is at least twice the frequency of the lowest torsional mode, this coupling effect is weak, and the longitudinal frequencies can be calculated as if there were no torsional restraint from the shaft system, and torsional frequencies can be calculated as if the system were infinitely rigid in longitudinal motion.

A simple example illustrating the effect is easily visualized. A spring and mass hung freely and set into vertical oscillation will acquire a rotational motion as well. If this spring-mass system is instead given a torsional oscillation, it will then soon acquire a vertical periodic movement.

In this example, the spring has a rotational "k_θ" as well as longitudinal mode "k_x" and they are interrelated by the construction of the spring. The case of the propeller-shaft system is analogous.

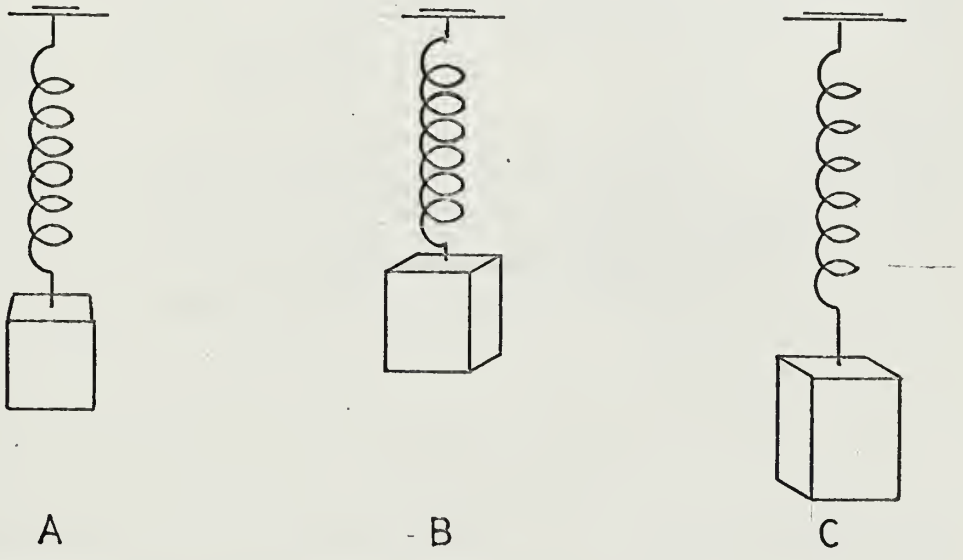

A. AT REST
B. SPRING COMPRESSED
C. SPRING IN TENSION

FIGURE III -10

Bending Vibration Modes.

The bending mode is also coupled to the torsional and longitudinal modes of vibration through the water inertia and damping of the propeller. As in the longitudinal-torsional case, this coupling should not be a serious concern if the natural frequencies of the modes are far apart (or out of the operating range of the system).

However, there are two modes of bending motion which may be expected. One mode is the bending of the measuring unit shaft because of exciting moments generated by the propeller. See figure III-11.

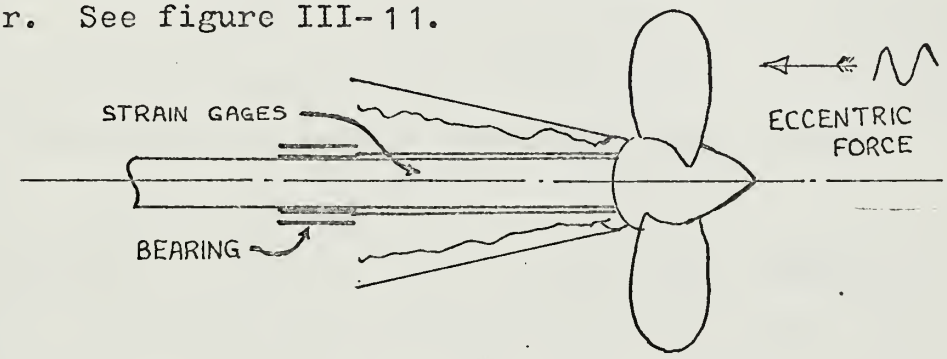

FIGURE III -11

The other mode is bending vibration of the entire shaft and housing assembly. See figure III-12.

FIGURE III -12

One mode may excite a harmonic of the other mode. See appendix for an analysis of the expected natural frequencies.

Data Collection and Analysis.

The blade generated forces are sensed by the strain gage matrix located immediately upstream of the propeller. Since the shaft is quite stiff, even at the strain gages, it is necessary to provide amplification of the signals to provide a detectable output. Amplification is done by integrated circuit operational amplifiers located inside the measuring unit shaft. A gain of approximately 10^3 is given for all six bridge circuit outputs.

The amplified signals are carried by a 16 conductor cable which is led through the hollow drive shaft by two Lebow model 8116-8 slip ring units and then to a Northern Scientific NS-550 Digital Memory Oscilloscope. The NS-550 performs the signal averaging and stores the averaged signal for readout on command.

The NS-550 is fitted with a memory bank capacity of 1024 words, with each word having five characters. The memory may be divided into 1024, 512, 256, or 128 words to provide one, two, four or eight channels of storage. This feature will permit several options in the way the signals are averaged. Thus the memory may be divided into eight sections and six of them used for the six outputs and one for the timing pulse (one channel remains blank). Or, all of the memory may be used to provide a highly detailed look at only one signal. This would mean that there would be nearly 1024 points available to describe the output for the 360° of periodic signal. This kind of resolution would

permit determining harmonics to a very high order.

The NS-550 has associated with it an ASR-33 teletype and a tape punch/tape reader which forms an essential part of the data analysis system. The NS-550 will read out its memory on command to the TTY and tape punch. The TTY can be used as a time sharing console (with a Dataphone) to communicate with a large general purpose computer.

The data analysis function works like this:

1. Call up signal analysis program on the computer time sharing system using the AST-33 TTY and Dataphone.

2. On signal from the computer program that it is ready to receive data for analysis, command the NS-550 to commence reading out to the TTY. At the same time the read out is transmitted to the computer via the Dataphone. A paper tape may also be punched at this time to make a permanent record of the averaged raw data in case of program interrupt.

3. Upon completion of the readout, the console is used to execute the analysis of the data.

4. When analysis is complete, the computer will transmit the results back to the console.

The data readout is the most time consuming part of the data processing since the system is limited to 100 words per minute by the TTY. While awaiting the results of the analysis, a new run can be set up and the flow conditions allowed to stabilize if desired.

Signal Averaging The NS-550 divides an incoming signal into a number of segments equal to the number of words of memory allocated to the signal. Each segment is individually averaged and that average value stored in a memory unit assigned to that particular segment. This process is called digitizing the signal. The digitizing process begins only on receipt of a timing or synchronizing pulse.

A variable sweep rate setting determines the time it will take for the averager to digitize one cycle of an incoming signal. Each sweep is completed, regardless of the receipt of another sync pulse. This means that a sweep period slightly longer than the signal period must be chosen if an entire cycle is to be averaged. It also means that only every other cycle of a periodic signal will be averaged, since the timing pulse will arrive at the NS-550 while a sweep is in progress.

If desired, less than a full cycle of a periodic signal may be averaged. In this case, a sweep period which is shorter than the signal period is chosen and only the first part of every incoming signal will be averaged. The portion of the signal which is averaged will depend on the ratio of the sweep period to the signal period.

It is assumed that each signal fed to the NS-550 will consist of random noise and a periodic signal of interest. If the sync pulse marks the beginning of the periodic portion, and if the sync pulse is received after exactly the same time interval each time, the periodic portion will re-

peat itself exactly. The noise portion will not repeat exactly since it is random. If successive sweeps are digitized, added and stored, the signal of interest will build up in direct proportion to the number of sweeps, while the noise accumulates only as the square root of the number of sweeps.

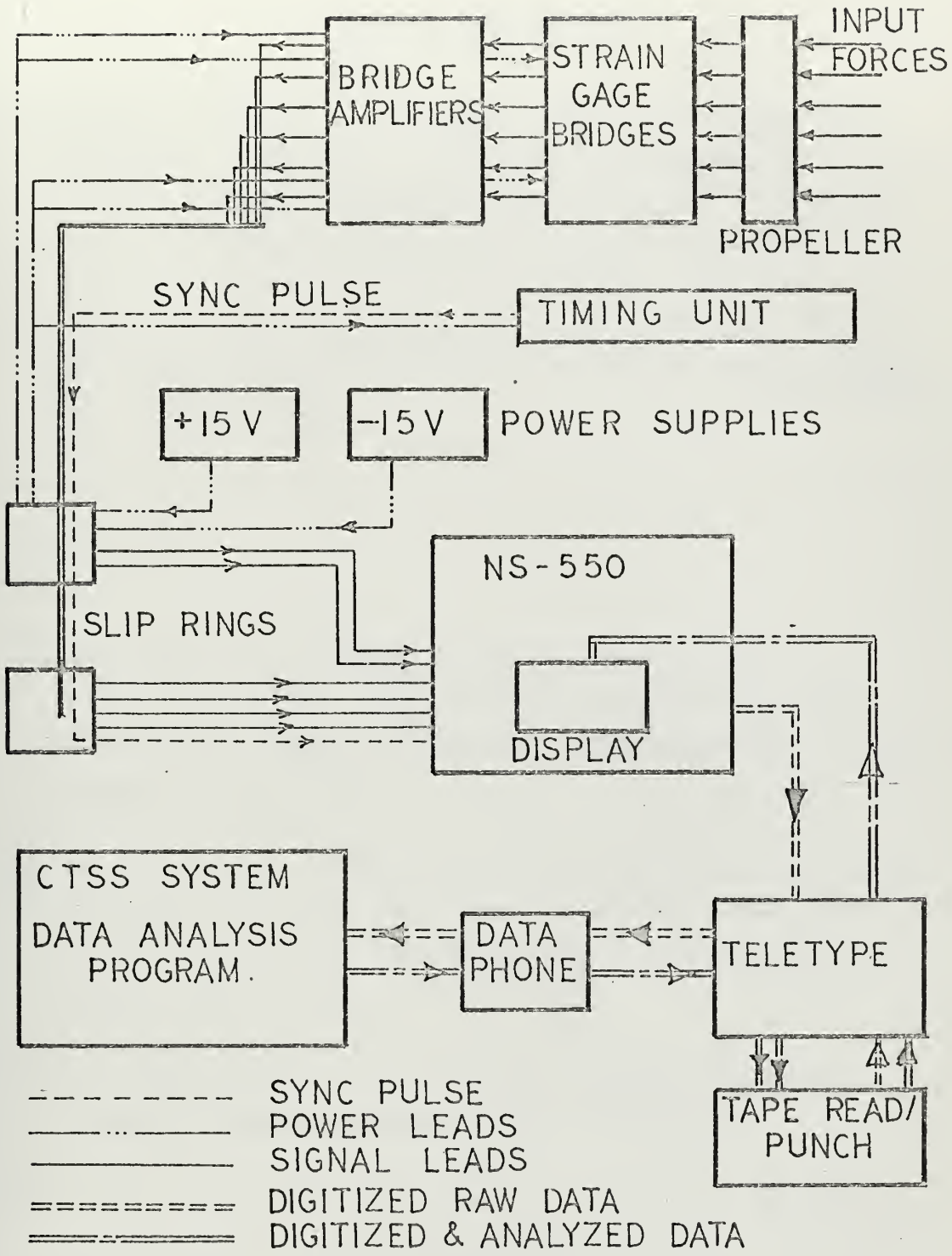

DATA ANALYSIS SYSTEM

FIGURE III -13

LIST OF REFERENCES

[1] Kerwin, Justin P., Cummings, D.E., and Wereldsma, Reinder, "Unsteady Hydrodynamic Measurements in the M.I.T. Variable Pressure Water Tunnel," A proposal to the National Science Foundation, July 1968.

[2] Lewis, Frank M., "Propeller Testing Tunnel at the Massachusetts Institute of Technology, Transactions, S.N.A.M.E., 1939.

[3] Ref. 2.

[4] Ref. 1.

[5] Tsakonas, S., Breslin, John P., and Miller, M., "Correlation and Application of an Unsteady Flow Theory for Propeller Forces," Transactions, S.N.A.M.E., 1967.

[6] Wereldsma, R., "Experimental Determination of Thrust Eccentricity and transverse Forces Generated by a Screw Propeller," International Shipbuilding Progress, Vol. 9, No. 95, July 1962.

[7] Trimble, Charles R., "What is Signal Averaging?" Hewlett-Packard Journal, April 1968, p. 2.

[8] Lewis, F.M. and Auslaender, J., "Virtual Inertia of Propellers," Journal of Ship Research, S.N.A.M.E., Vol. 3, No. 4, March 1960, p. 37.

[9] Brandau, John H., "Static and Dynamic Calibration of Propeller Model Fluctuating Force Balances," N.S.R.D.C. Carderock, Report 2350, August 1967, p. 55.

[10] Uhlig, H.H., Corrosion and Corrosion Control, New York: John Wiley and Sons, Inc., 1963.

[11] Ref. 10.

[12] Manen, Van, J.D., and Wereldsma, R., "Dynamic Measurements on Propeller Models," International Shipbuilding Progress, Vol. 6, No. 63, November 1959, p. 474.

[13] Den Hartog, J.P., Mechanical Vibrations, 4th edition. New York: McGraw-Hill Book Company, Inc., 1956, p. 225.

[14] Ref. 13, p. 229.

[15] Krohn, J., and Wereldsma, R., "Comparative Model Tests on Dynamic Propeller Forces," International Shipbuilding Progress, Vol. 7, No. 76, December 1960, p. 533.

[16] Ref. 13, p. 396.

[17] Ref. 8, p. 43.

[18] Noret, Ronald, "Deadweight Calibration of Strain Gage Bridges on Measuring Shaft," Charles Stark Draper Laboratory Memorandum Report, March 23, 1970.

[19] Ref. 9, p. 15.

APPENDIX A - SENSOR CALIBRATION

Static Calibration.

A series of static calibrations, done by hanging weights on the propeller mounting taper to simulate pure thrust, torque, side forces and bending moments will provide correlation between propeller generated forces and strain gage outputs. "Cross talk" which is output from one strain gage bridge caused by a force applied to excite another bridge must also be determined. The results of all static calibration series can be grouped into a six matrix of influence coefficients.

Ideally, each strain gage bridge would measure only the input force or moment that it is supposed to measure and would have no output when other forces, moments or combinations are applied to the shaft. The matrix of influence coefficients would be diagonal and when written in equation form would look like

$$\begin{bmatrix} g_1 \\ g_2 \\ g_3 \\ g_4 \\ g_5 \\ g_6 \end{bmatrix} \begin{bmatrix} 1 & 0 & 0 & 0 & 0 & 0 \\ 0 & 1 & 0 & 0 & 0 & 0 \\ 0 & 0 & 1 & 0 & 0 & 0 \\ 0 & 0 & 0 & 1 & 0 & 0 \\ 0 & 0 & 0 & 0 & 1 & 0 \\ 0 & 0 & 0 & 0 & 0 & 1 \end{bmatrix} = \begin{bmatrix} T \\ V \\ H \\ Q \\ M_h \\ M_v \end{bmatrix} \qquad (1)$$

Equation (1) says that the output of bridge 1, represented by g_1, gives the entire thrust output. The same condition holds for the other forces and the three moments.

In actuality, there will be other non-zero influence coefficients besides these on the diagonal and that matrix of influence coefficients will look like

$$\begin{matrix} a_{11} & a_{12} & a_{13} & a_{14} & a_{15} & a_{16} \\ a_{21} & a_{22} & a_{23} & a_{24} & a_{25} & a_{26} \\ a_{31} & \cdot & \cdot & \cdot & \cdot & \cdot \\ \cdot & & & & & \cdot \\ \cdot & & & & & \cdot \\ a_{61} & \cdot & \cdot & \cdot & \cdot & a_{66} \end{matrix}$$

In equation form, the influence coefficients and gage outputs combine to look like this.

$$a_{11}g_1 + a_{12}g_2 + a_{13}g_3 + a_{14}g_4 + a_{15}g_5 + a_{16}g_6 = T \qquad (3)$$

Equation (3) says that each of the gage bridge outputs must be multiplied by its influence coefficient and summed to determine the actual thrust input to the sensor. There are a total of six equations, each with up to six terms. Some of the influence coefficients may be zero, however.

Dynamic Calibration.

If the sensor were to be used for static low frequency inputs, a static calibration would be all that is required for reliable and consistent results. This is not true in the dynamic case however, since some input frequencies to the sensor may excite natural frequencies in the sensor itself. In such a case, a very low magnitude input from the propeller (say a 2^{nd} or 3^{rd} harmonic of a blade vibration) to the sensor will cause an unusually large output from the sensor. The resonant elastic strains would be of much higher magnitude than non-resonant ones and of course a disproportionate signal would be generated by the bridge networks. Therefore, a dynamic calibration, similar to the one described by Brandau [9] must be done to have confidence in experimental results.

Such a dynamic calibration should cover a frequency range from the lowest anticipated propeller RPM up to a few harmonics above the highest expected blade frequency. Or, between the limits of

$$500 \text{ RPM} = 80 \text{ cps}$$

and

$$\frac{2000 \text{ RPM} \times 9 \text{ Blades} \times 3 \text{ Harmonics}}{60 \text{ sec/min}} = 900 \text{ cps}$$

if only a third harmonic of a nine bladed propeller is the highest expected frequency input.

The calibrations done on the NSRDC sensor described

in [9] were between the frequencies of 50-1450 cps. A resonance in the torque output caused sensor response in the side force, moment and thrust bridge networks. Thus, the cross talk between networks is also frequency dependent because of mechanical coupling in the sensor construction.

The result of a complete dynamic calibration will be a family of calibration matrices, with each member of the family similar to the matrix shown as equation (2). Individual terms will vary from matrix to matrix according to frequency.

If these variations are smooth, it should be possible to develop a functional relationship between the bridge network output for each force signal and the frequency of that output, and incorporate this feature into the analysis program.

The set of signals from the NS-550 should be analyzed for frequency content (Fourier Transformed) prior to being run through the calibration matrix family, since the gage outputs are frequency dependent. They will all be harmonics of the synchronizing frequency, (shaft RPM) but will not necessarily be the same harmonic.

If this feature is not programed, considerable manual computation effort will be required. After the frequency content of a signal is determined, it will be necessary to look up an amplitude factor for that gage bridge at that particular frequency. This factor can then be treated as the a_{ij} in the static calibration matrix

and the true magnitude of the signal can be determined. This will have to be done for each harmonic of each output signal for all six signals.

Frequency response of the strain gage sensor is affected by the inertia of the mass attached to it. Since the inertia of the dynamic calibration shakers and the model propellers will not be the same (especially in all six degrees of freedom), it is hoped that the inertial effects on frequency response will prove to be negligible.

APPENDIX B - CONTROL OF CORROSION

The tunnel is constructed entirely of mild steel. Most of the structural parts are rather thin, so rusting of the walls is not permissable, even if the resulting cloudiness of the water could be tolerated. The most practical way to prevent rusting of the tunnel walls is to remove dissolved oxygen from the water.

An addition of sodium sulfite to deactivate the tunnel water has proved effective for several years. The oxygen is removed in accordance with the reaction.

$$Na_2SO_3 + \tfrac{1}{2}O_2 \text{ ---- } Na_2SO_4$$

in which Na_2SO_3 reacts with in the ratio of 8 lbs. Na_2SO_3 for every 1 lb. of dissolved oxygen. The reaction is slow at ordinary temperature but can be speeded up by adding Cu^{++} or Co^{++} as catalysts [10].

The addition of Na_2SO_3 makes the tunnel water toxic and also affects the corrosion resistance of aluminum and aluminum alloys, since aluminum depends in part on the prescence of dissolved O_2 to create a passive oxide film.

"Traces of Cu^{++} (as little as .1 ppm) or Fe^{+3} in water are effective in breaking down passivity of aluminum. Galvanic cells are formed between Al and the deposited metallic Cu or Fe (by a replacement reaction) which stimulates the dissolution of Al at local areas" [11]. Because of the mild steel tunnel construction and the use of brass and bronze parts for experimental apparatus it can be assumed that there are adequate quantities of both

Cu and Fe ions to cause pitting of aluminum parts used in experiments.

In practice, aluminum propellers and other experimental parts have been used in the past. Prolonged exposure to the tunnel water (24 hours or more), however, leads to severe surface corrosion.

APPENDIX C - PREDICTED MODES OF VIBRATION AND NATURAL FREQUENCIES

Acceptable Natural Frequencies.

If experience with the two degree of freedom propeller testing system is applicable to the six degree of freedom system, it will not be necessary to operate the shaft at over 2000 RPM to get desired levels of output from the propeller.

At 2000 RPM and using a 7 bladed propeller, a blade frequency of 14000 cpm or 233 cps is generated. If one is interested in no higher than the third harmonic, a frequency of 700 cps must be sensed by the system.

In order to keep the magnification factor near unity and the phase angle near zero, the system should be operated at an RPM which gives blade frequencies sufficiently far from interfering natural frequencies. See figure C-1.

Figure C-1 is an expanded version of figure III-2, which shows the relationship between ω, ω_n, system response amplitude and damping. Figure C-2 shows a similar relationship for the phase angle.

Analytical estimates of system damping are difficult to accurately determine. Wereldsma in [12] states that c/c_c is less than 0.6. However, estimates of c_c from $c_c = 2\sqrt{km}$, indicate that c/c_c should be much smaller, perhaps on the order of 0.02. Estimates of system damping can be made much more accurately by observation of the phase angle behavior while the system is in operation.

If the value of c/c_c = .02 is approximately correct, choosing ω/ω_n less than or equal to 0.2 will restrict the M.F. to less than or equal to 1.04 and will keep it in a nearly linear growth range (See figure C-1). Such a choice of maximum ω/ω_n will also keep the maximum phase angle less than one degree.

Can the choice of ω/ω_n = .2 be reasonably met, given the system physical dimensions? Using a maximum of seven blades and running a test at a maximum of 2000 RPM, no system natural frequencies below

= 700/.2 = 3500 cps could be permitted.

If only the second harmonic is of interest, a lower limit on the permissable natural frequency can be tolerated in the system.

= 467/.2 = 2333 cps

More propeller blades and higher RPM's would of course dictate more stringent restrictions on permissable natural frequencies. The remaining sections of this appendix discuss estimations of expected natural frequencies for several possible modes of vibration.

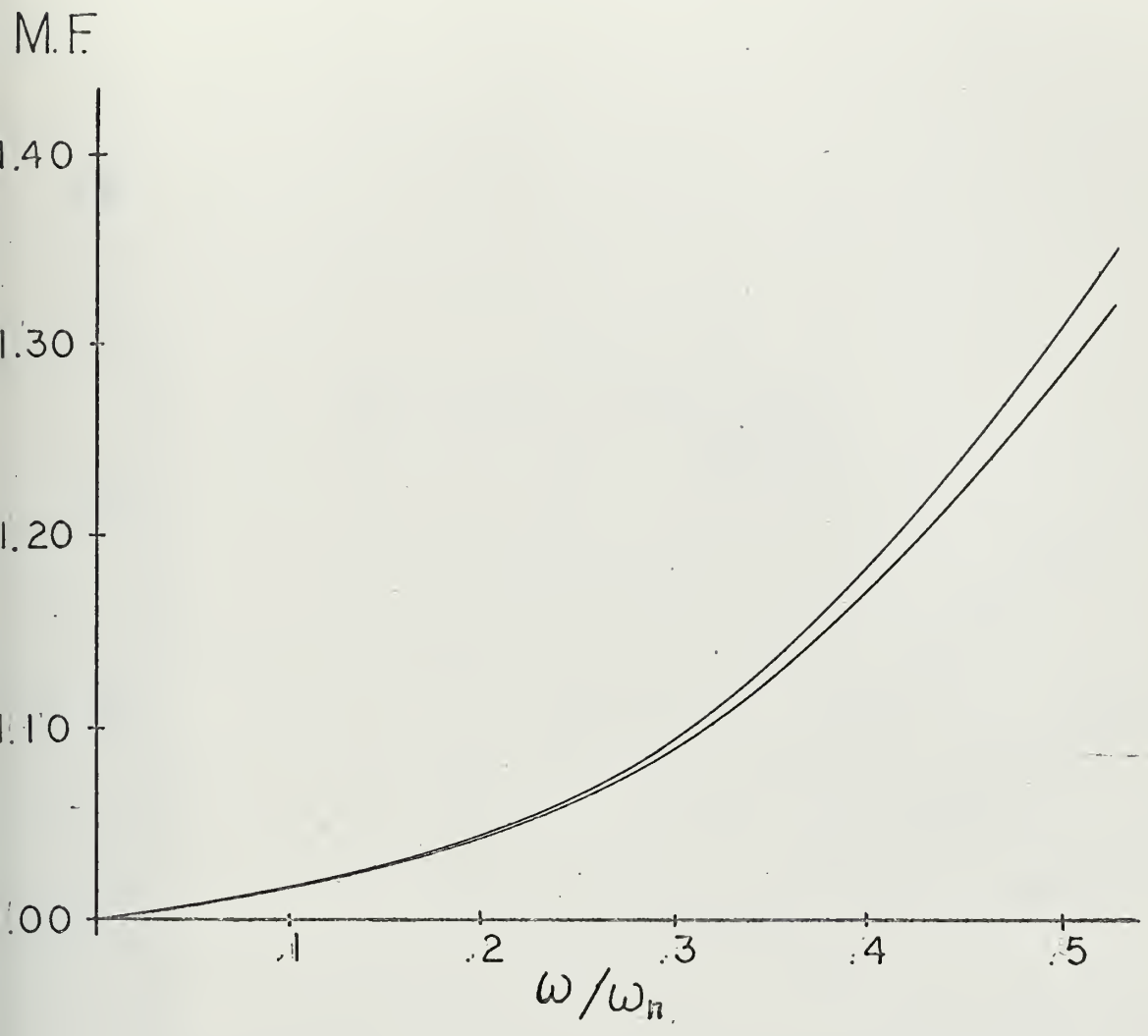

MAGNIFICATION FACTOR vs FREQUENCY RATIO

FIGURE C-1

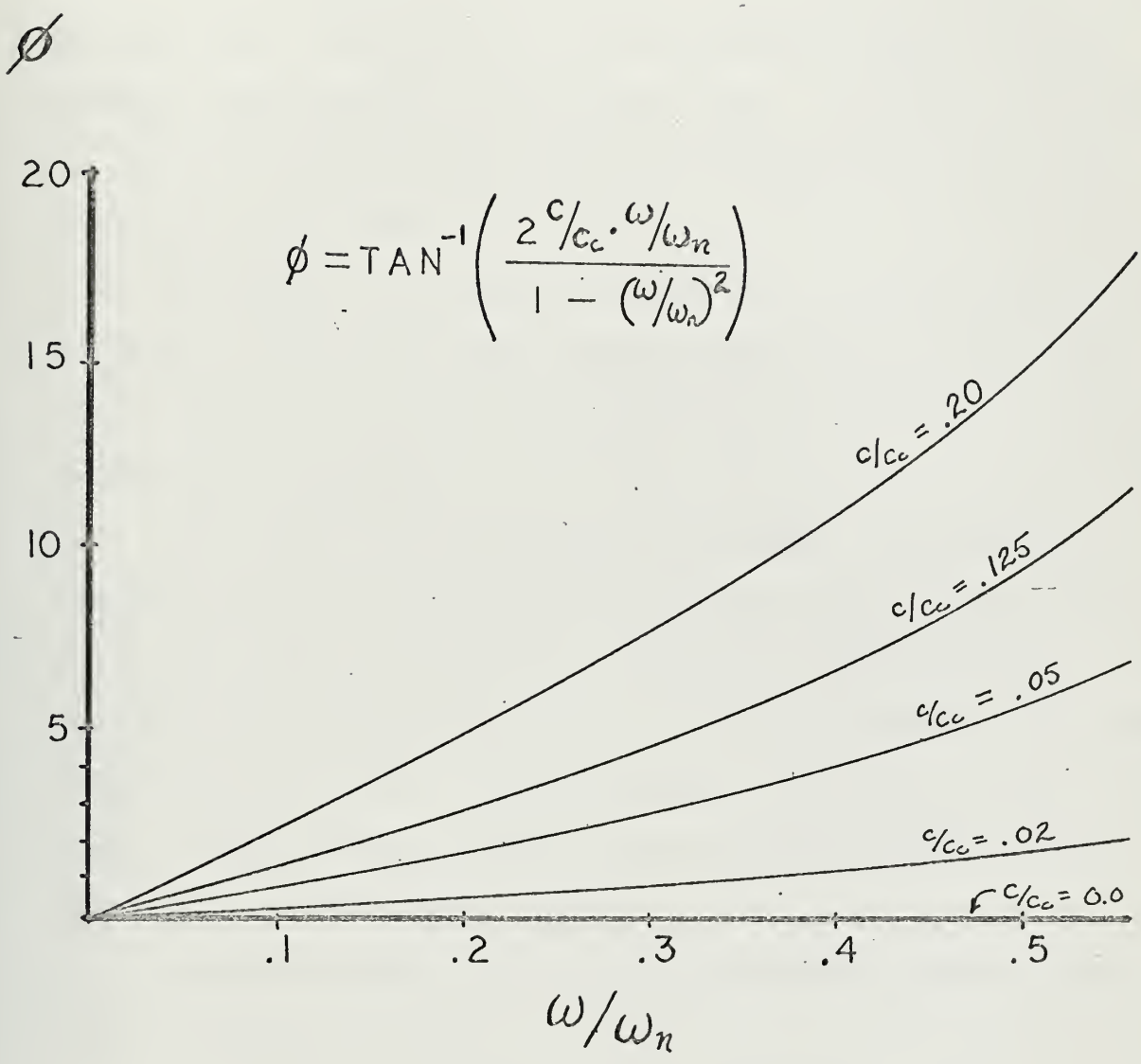

PHASE ANGLE vs FREQUENCY RATIO

FIGURE C-2

Critical Shaft Speeds.

Critical shaft speeds occur in rotating machinery because of eccentricity of loading. If a mass is rotating on a shaft and its center of gravity does not coincide with the shaft axis of rotation by a distance e, called the eccentricity, there will be one rotational speed at which violent oscillations will tend to occur. At RPM's far above or far below this critical speed, deflections of the shaft will not be serious.

In general, the critical speed (or critical speeds if there is more than one rotating mass) will be the same as the natural frequencies of vibration of the shaft held by two rigid bearings.

The intent in constructing the shaft and measuring system is to balance all major rotating parts and to carefully align the axes so that off-center weights between bearings will be minimized, but it can be expected that some unbalance will occur. In particular, the effect of the signal leads passing through the drive shaft must be considered as an off center weight.

In the consideration of critical shaft speeds, notation is fairly standard.

B = The center of the bearings

S = The center of the shaft at the weight

G = The center of gravity of the weight

e = The constant distance between S and G (eccentricity)

r = $\overline{BS}$ = the deflection of the shaft at the mass

A physical model of this situation looks like figures C-3 and C-4. The off center mass is shown as a disk. At rest S and B will approximately coincide; G will be off center a distance e.

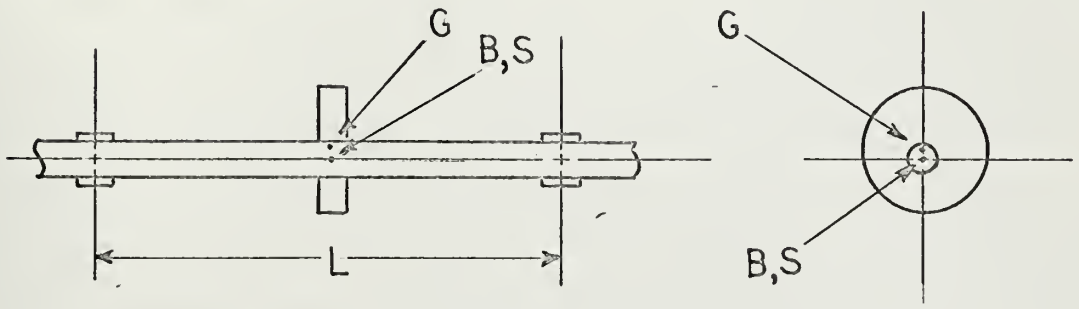

FIGURE C - 3

When rotating at a speed below the critical speed, the inertial effect of the rotating off center mass will cause the shaft to deflect until the inertial force is balanced by the restoring force of the elastically bent shaft.

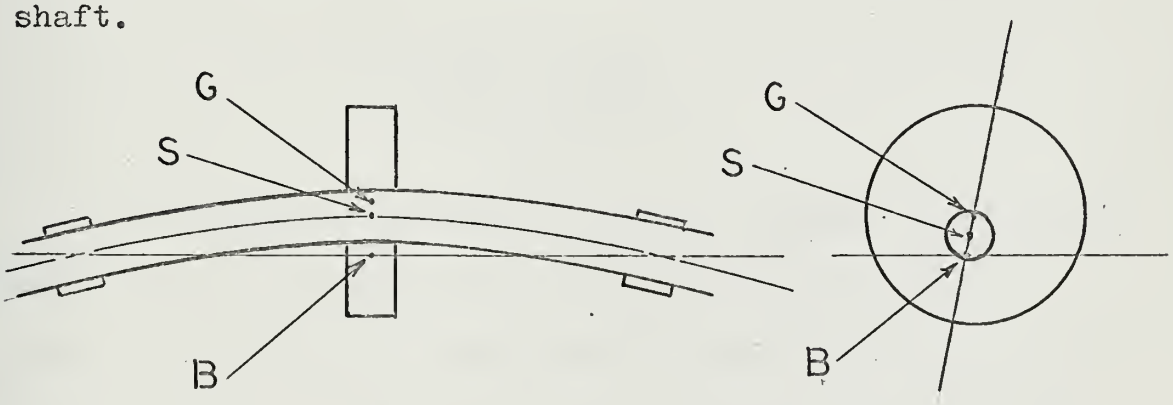

FIGURE C-4

While the shaft is rotating below the critical speed, the only stable configuration is for points B, S and G to be

collinear. At the critical speed, the shaft deflection $\overline{BS}$ becomes very large. Above the critical speed, the Coriolis acceleration drives G back toward B and causes the shaft to become stable once more. The further above critical speed, the more stable the shaft becomes. However, if the collinearity of the three points is enforced as the critical speed is passed then G cannot escape around S to coincide with B, and the system will remain unstable. See Den Hartog [13] or another text on mechanical vibration for a full discussion of the effect. The critical frequency (cps) for the simple model shown in figures C-3 and C-4 is given by the equation

$$\omega_n = \sqrt{k/m}$$

Where $M = \frac{W}{g}$, W = weight of off center mass.

$$k = \frac{48EI}{L^3} \qquad I = \frac{\pi}{64}\ (D_o^4 - D_i^4)$$

$$k = \frac{3\pi E\ (D_o^4 - D_i^4)}{4L^3}$$

An accurate consideration of the natural frequencies would require a method of successive approximations similar to the Holzer method of torsional analysis to account for the effect of distributed mass in the real shaft[14]. Instead, some reasonable guesses will be made to compute natural frequencies for the potentially most critical situations.

For the drive shaft, with axial distance between bearing centers equal to 34 inches,

$L = 34$ $\qquad E = 29.5 \times 10^6$

$D_o = 1.75$

$D_i = 1.54$ $\qquad k = \dfrac{(3)\ (29.5)\ (3.75)\ 10^6}{(4)(34^3)} = 6640$ lb/in

The weight of a 3 foot section is approximately 6 lb. and the weight of 3 feet of signal lead at approximately 27 grams/ft is .172 lb. The maximum weight between bearing centers is then approximately 6.2 lb. Assuming that this total weight is all off center (a grossly exaggerated assumption), find

$$\omega_n = \sqrt{\frac{6640}{.01605}} \qquad m = \frac{6.2}{386.2}$$

$\omega_n =$ 102 cps $\qquad m = .01605$

$\omega_n =$ 6120 RPM

With a much smaller off center weight (which is more reasonable), say on the order of .5 lb,

$$\omega_n = \sqrt{\frac{6640}{.00129}} \qquad m = .00129$$

$\omega_n =$ 362 cps = 21700 RPM

Thus normal shaft RPM should be well below the critical speed.

This is probably still much too low, since the cable weight is distributed across the shaft section and not concentrated at a point, so the effect of the cable weight is even less than computed above and the frequency should be higher.

Bending Vibrations.

The measuring unit shaft has a varying sectional area. To accurately compute the natural frequencies, the shaft must be treated as a distributed mass instead of a collection of lumped masses connected by massless springs.

It was decided that approximations would suffice for first investigations of system response, especially since interaction of the components was difficult to predict in advance. Accordingly, the following calculations and assumptions attempt to model the actual situation with sufficient accuracy determine potential problem areas for more detailed analysis, if required.

Sensor Mounting Natural Frequency. The strain gage mounting itself has a varying cross section as well as a varying moment of inertia which depends on the angle of rotation.

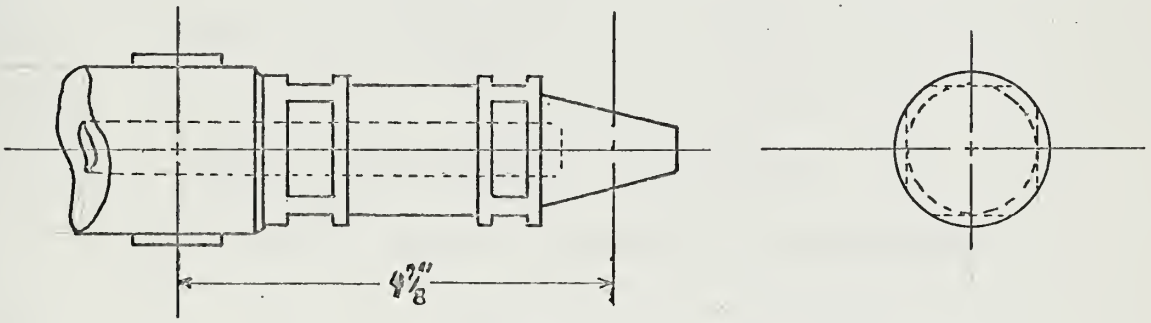

FIGURE C-5

Assume that the portion of the shaft containing the

gages has an effective section 1.5 inches in diameter with a .50 inch hole, and that it will vibrate as a cantilever from the center of the bearing through the center of the propeller mounting taper. This assumption of an effective O.D. of 1.5 inches will provide the smallest K, hence the lowest natural frequency estimate for this mode of vibration. Such an assumption is probably not too inaccurate since holes for the strain gage leads are drilled through the wider section near the bearing which reduces the effective section area at the wider cross section.

For a cantilevered beam, transverse loading

$$k = \frac{3EI}{L^3} \qquad I = \frac{\pi}{64}(D_o^4 - D_i^4)$$

$$k = \frac{3(29.5)\ (.2445)\ 10^6}{4.87^3} \qquad I = .2445\ \text{in}^4$$

$$k = .188 \times 10^6$$

$$m = \frac{\text{propeller weight}}{386.2} = \frac{10}{386.2} = \frac{.0259\ \text{lb-sec}}{\text{in}}$$

$$\omega_n = \sqrt{\frac{.188 \times 10^6}{.0259}}$$

$$\omega_n = 2695\ \text{rad/sec} = 429\ \text{cps}$$

This frequency can be expected to be somewhat lower than the estimated 2700 cps because the effect of mass of the shaft has been ignored.

A different shaft stiffness must be used for moment excited vibrations.

$$k = \frac{2EI}{1^2} = \frac{2(29.5 \times 10^6)\ (.2445)}{4.87^2}\ \text{lb}$$

$$k = .609 \times 10^6\ \text{lb}$$

If exciting moments are on the order of five percent of the torque, as indicated in [15], a natural frequency of

$$\omega_n = \sqrt{\frac{.609 \times 10^6}{5/386.2}}$$

$$= 3065\ \text{rad/sec} = 488\ \text{cps}$$

should be expected.

Since the shaft is far stiffer in other areas, other bending mode natural frequencies in the measuring unit shaft and flywheel assembly should be significantly higher and thus of no concern.

In the general area of bending frequencies, two other factors are of design concern. One is the inclusion of a soft bearing support near the flywheel to absorb transverse motions of the shaft (or transverse motions of the housing assembly). Accurate prediction of the behavior of this feature under dynamic circumstances is difficult at best.

The other concern is the motion of the shaft and housing together. Such motions may not be detremental

(in principle) to the measurements being taken, but if extreme, they could be damaging to the system as a whole.

Bending of Shaft and Shaft Housing. The shaft and housing for the six degree of freedom system are similar in construction to the two degree of freedom system and are supported in exactly the same way. Knowledge of the vibration behavior of the old system can therefore be used to predict behavior of the new shaft.

The old shaft passes through a resonance between 350 and 400 RPM (58-66 cps). It is expected that the new shaft should also have a resonance somewhere near this range, since bending mode vibrations are a function of shaft length and diameter. They are independent of section area, E, and I [16]. The amplitude of such vibration may differ between the two shafts because of loading differences, but this should be of little consequence, since the resonant shaft RPM is far from the expected range of operation.

Torsional Vibrations.

External torsional vibrations of the system are not isolated from the strain gages except by the flywheel. There are no "soft" torsion transmitting devices in the drive train to the propeller. The drive shaft itself does act, however, somewhat like a torsion vibration absorber by virtue of having a torsional stiffness an order of magnitude smaller than the rest of the shaft system. Table C-1 shows the torsional stiffnesses of several sections of the of the drive shafting.

TABLE C-1

Shaft Section	k_θ (rad/in-lb x 10^6)
drive shaft	.234
flywheel	11.11
amplifier section	5.78
middle section	4.51
sensor gage mounting	2.06

A FORTRAN computer program using the Holzer method of analysis was written and used to determine the approximate torsional natural frequencies. A description of the program is contained in Appendix D.

A few models, more simple than the one used in the program are instructive to consider in investigating the expected system vibration behavior.

The purpose of the flywheel as originally conceived was to act as a stable reference, or literally a ground for the sensor. A large mass and inertia would appear quite stable to the sensor shaft in all three modes of vibration. If the flywheel were also isolated from excitation other than via the propeller forces and moments, the signals generated by the strain gages would be due entirely to the propeller generated forces and moments, and the system natural frequencies should be high enough or low enough to be well out of the operating range. However, as was pointed out earlier, the size of the flywheel (and with it,

its mass and inertia) was sacrificed for reasons of operating convenience, economics and to provide a smooth propeller inlet flow. This reduction in effectiveness of the flywheel was felt to be a justifiable tradeoff.

Theoretical or experimental estimates of model propeller rotational inertias are not readily available. Lewis and Auslaender [17] quote a 1955 thesis by R. J. Price for a value of J_Θ of .000588 lb-ft^2 which includes the added mass effect. Very approximate estimations for J_Θ for a non-operating bronze propeller with five blades and a weight of 10 lb give J_Θ's in the range of .2 to .3 lb-in-sec^2. This does not compare closely with the value of .0847 lb-in-sec^2 determined by Price when the units are made compatible.

Because of the uncertainty of the actual value of J_Θ for typical model propellers, and the likelihood of using several different propellers of different masses and sizes in future tests, it is necessary to do natural frequency estimations for several values of J_Θ for the propeller. The flywheel inertia, J_f, was kept constant during the calculations.

J_p = rotational inertia of the propeller

Assume that $.01 \leqslant J_p \leqslant .25$

Now compute the inertia of the flywheel:

$$J_f = \frac{m}{8}(D_o^2 - D_i^2) = \frac{27.5}{(8)(386.2)}(3.40^2 - 1.45^2)$$

$$J_f = .0842 \text{ lb-sec}^2\text{-in}$$

In the measuring unit shaft, flywheel, and propeller assembly, there are five more or less distinct inertial masses and theoretically five degrees of freedom. The masses and stiffnesses of the shaft are sufficiently close in value to each other that the system can be represented as two inertial masses connected by an average stiffness, and the inertia of the shaft itself can be neglected. A diagram of this approximation is shown in Figure C-6.

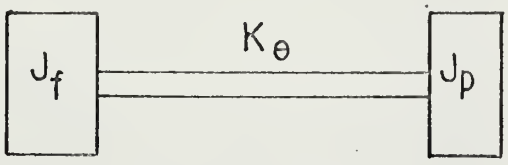

FIGURE C-6

where $$\omega_n = \sqrt{\frac{k_\theta (J_p + J_f)}{J_p J_f}}$$

A series of computer calculations using the above figures for D_o and D_i with $J_f = .0842$ resulted in values for the curve of natural frequency versus J_p shown in Figure C-7. The assumed value of shaft stiffness, $k_\theta = 5.0 \times 10^6$ gave a predicted range of natural frequencies which are quite high and should be well out of the operating range.

The torsional analysis program using the Holzer method treated each portion of the measuring unit assembly with a different cross section as a distinct inertial mass. It indicated that the expected natural frequency should be much lower than any shown in Figure C-7. The Holzer method

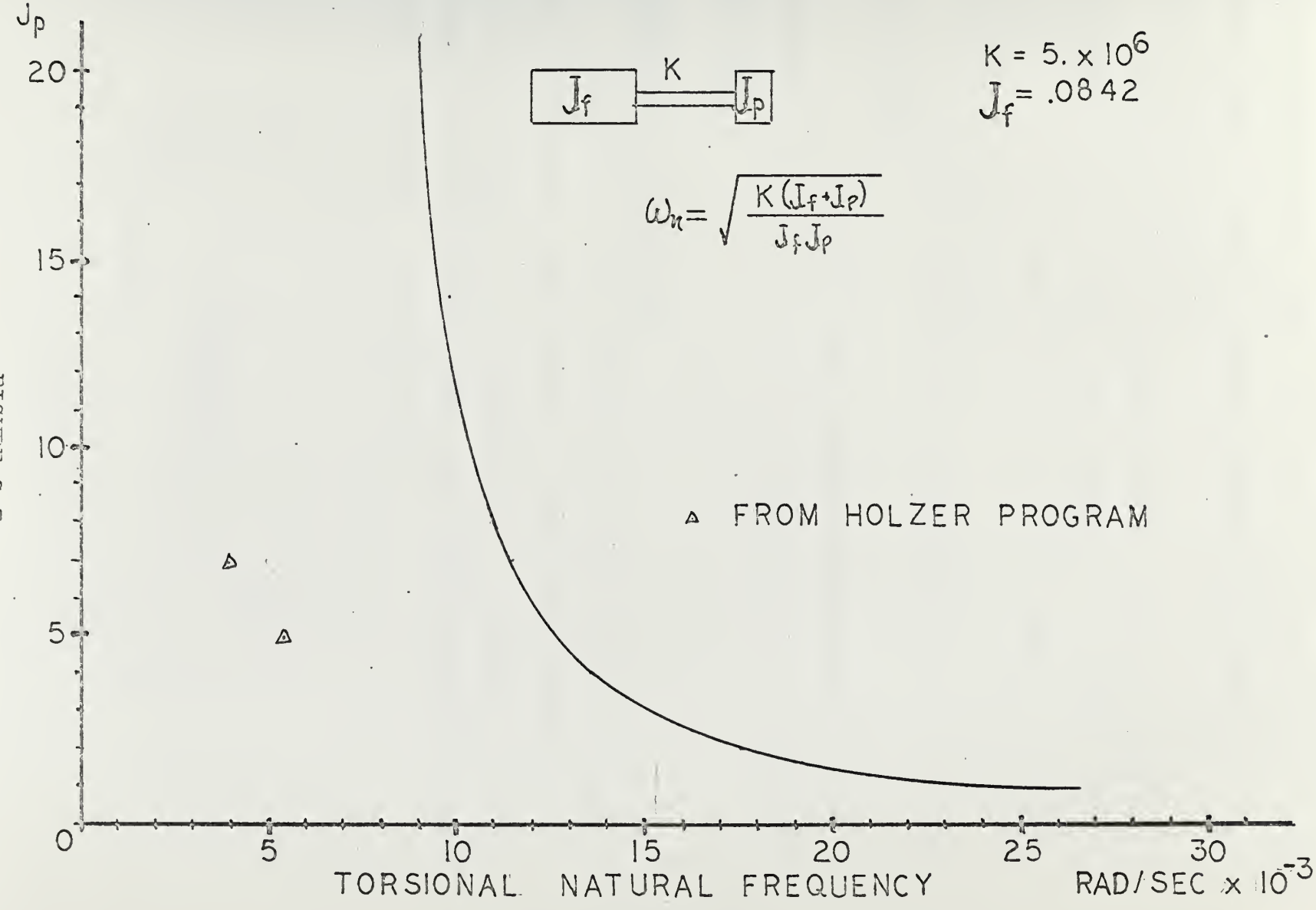
J_p
20
15
10
5
0
J_f
K
J_p
$K = 5. \times 10^6$
$J_f = .0842$
$\omega_n = \sqrt{\frac{K(J_f + J_p)}{J_f J_p}}$
△ FROM HOLZER PROGRAM
5
10
15
20
25
30
TORSIONAL NATURAL FREQUENCY
RAD/SEC x 10^{-3}

FIGURE C-7

program predicted a natural frequency in the vicinity of 5450 radians/second (867 cps) for an assumed propeller inertia of .05. A higher natural frequency is possible if J_p can be further reduced.

Assuming that the methods and the results of the two calculations are correct, the difference in results imply:

1. the inertial effect of the shaft is not negligible in making estimations

2. the assumed shaft stiffness $k_\theta = 5 \times 10^6$ may be too high

3. the torsional analysis program results are probably more reliable, since fewer simplifying assumptions are made

Longitudinal Vibrations.

Two models of the shaft longitudinal vibration behavior are of interest. One is used to treat the measuring unit as being isolated by the flywheel and to estimate a natural frequency for the sensor shaft both with and without a propeller attached. See Figure C-8.

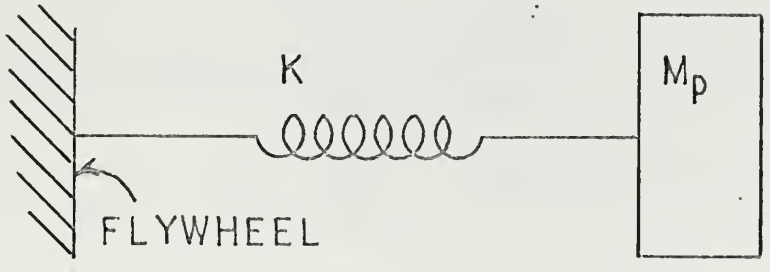

FIGURE C-8

The other model (Figure C-9) is used to treat the case of longitudinal vibrations in the drive shaft with the fly-wheel, measuring unit shaft and propeller being treated as a single combined mass.

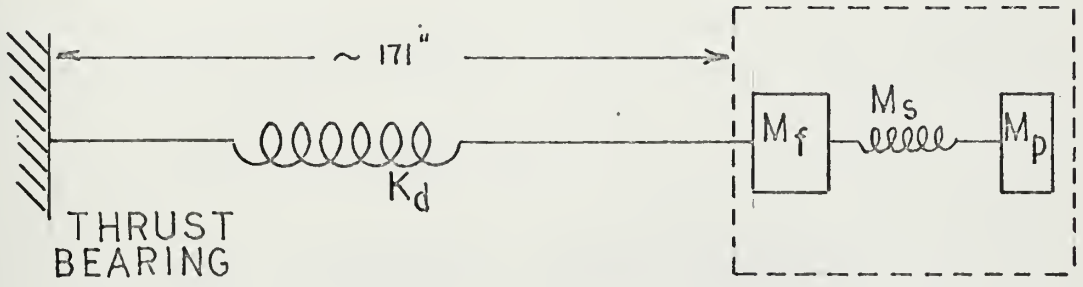

FIGURE C-9

Without a propeller, the ω_n for the measuring unit shaft is given by

$$\omega_n = (n + \tfrac{1}{2})\pi \sqrt{\frac{AE}{m_s l}}$$

where A = cross section area of sensor

$$= \frac{\pi}{4}(1.5^2 - .5^2) = \frac{\pi}{2} = 1.57 \text{ in}^2$$

m_s = mass of shaft = 8.0 lb/386.2

l = 12.2 inches

$$\omega_n = (n+\tfrac{1}{2})\pi \sqrt{\frac{(3.16)(29.5)10^6}{(.0282)(12.2)}}$$

$$= (n + \tfrac{1}{2})\pi \; 13{,}600 \text{ rad/sec}$$

$$= (n + \tfrac{1}{2}) \; 6800 \text{ cps}$$

ω_n = 10,200 cps for the fundamental

Other modes will be higher than this by an amount of 6800 cps for each additional harmonic.

With a propeller, the formula

$$\omega_n = \sqrt{\frac{k_s}{m_p + m_s/3}}$$

applies, with k_1 given by

$$k_s = \frac{AE}{l} = 3.80 \times 10^6$$

$$m_p = 10 \text{ lb}/386.2 = .0259 \text{ lb-sec}^2/\text{in}$$

$$\omega_n = \sqrt{\frac{3.80 \times 10^6}{.0259 + .0207/3}} = \sqrt{116 \times 10^6}$$

$$\omega_n = 10{,}760 \text{ rad/sec}$$

Considering the model shown in Figure C-9, compute the longitudinal stiffness of the drive shaft.

$$k_d = \frac{AE}{l} = \frac{(1.754^2 - 1.54^2)(29.5 \times 10^6)}{(4)(171)}$$

$$= .92 \times 10^5$$

$$M = m_f + m_s + m_p$$

$$= (27.5 + 8.0 + 10.0)/386.2 = .118$$

$$\omega_n = \sqrt{\frac{.92 \times 10^5}{.118}} = \sqrt{7.80 \times 10^4}$$

$$= 883 \text{ rad/sec} = 140.5 \text{ cps}$$

Effect of Predicted Natural Frequencies on System Operation.

Let us now list the predicted natural frequencies and their modes and consider the effects.

Bending	Approximate ω_n
Cantilever of sensor, side force excited	730 cps
Cantilever of sensor, moment excited	488 cps
Shaft and housing	60 cps
Torsional Vibration	
Two inertia model, measuring unit shaft	1430 cps
Holzer analysis, measuring unit shaft	867 cps
One inertia model, drive shaft	172 cps
Longitudinal Vibration	
Measuring unit shaft, no propeller	6800 cps
Measuring unit shaft, with propeller	1710 cps
Drive shaft and flywheel	140 cps

The expected range of frequencies of interest is determined by the shaft RPM, the number of blades on the model propeller being tested, and the number of harmonics which have a significant magnitude. The third harmonic of the blade frequency is the maximum expected to be detectable. Figure C-10 shows the relationship between RPM, number of blades and harmonics, and plots the expected occurrence of natural frequencies. It should be noted that several fall in the expected range of operation.

The potential serious conflicts which may be resolved are

1: 172 cps; longitudinal mode, thrust excited;

2: 140 cps; torsional mode, torque excited; and

3: 867 cps; torsional mode, torque excited.

Case 1 and 2 both involve the drive shaft-flywheel. In case 1, the longitudinal mode, the frequency can be changed by installing a thrust bearing nearer the flywheel, thus shortening the drive shaft "spring" and making it much more stiff.

Case 2, the torsional vibration of the drive shaft-flywheel may exist, since there is no built-in support in the rotational direction at the end of the drive shaft. The inertia of the drive pulleys and drive motor approximates such a built-in support, but the flexibility of the drive belts may be sufficient to damp any torsional vibrations in this mode.

Case 3, the torsional vibration of the sensor shaft itself constitutes a potentially serious problem. Since the sensor shaft cannot be modified without a major change and disassembly of the entire system. The only remaining alternative is to use propellers with a much smaller J_Θ. Aluminum propellers are commonly used in other installations to mitigate this same type of problem. The reduction in J_Θ is very small, however, and in addition, aluminum has a corrosion problem in the oxygen-free tunnel water.

Professor F. M. Lewis, of MIT has recently developed a process to accurately manufacture very lightweight and very

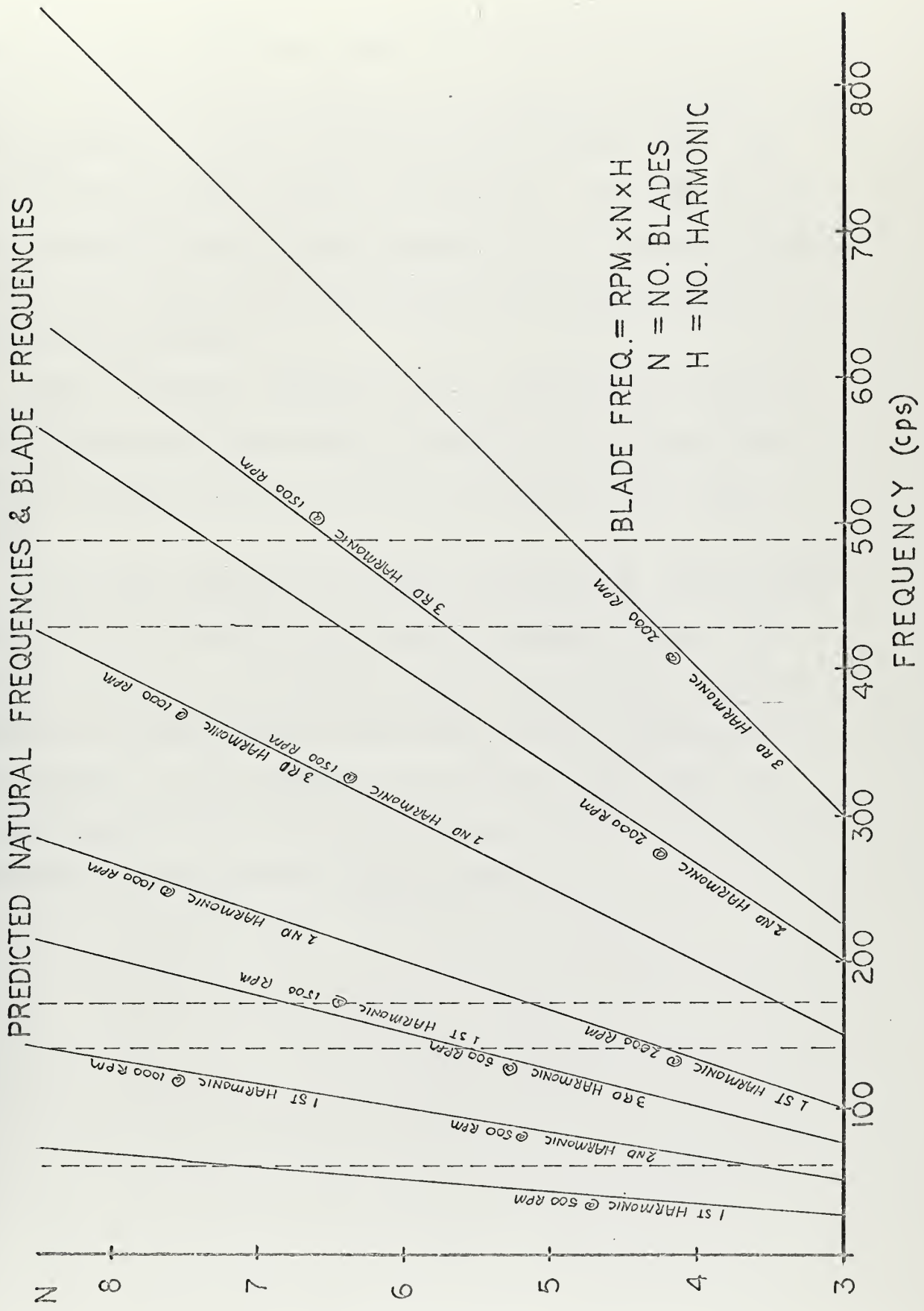
PREDICTED NATURAL FREQUENCIES & BLADE FREQUENCIES
BLADE FREQ. = RPM x N x H
N = NO. BLADES
H = NO. HARMONIC
FREQUENCY (cps)
100
200
300
400
500
600
700
800
N
8
7
6
5
4
3
1 ST HARMONIC @ 500 RPM
2ND HARMONIC @ 500 RPM
3RD HARMONIC @ 500 RPM
1 ST HARMONIC @ 1000 RPM
2 ND HARMONIC @ 1000 RPM
3RD HARMONIC @ 1000 RPM
1 ST HARMONIC @ 1500 RPM
2 ND HARMONIC @ 1500 RPM
3RD HARMONIC @ 1500 RPM
1 ST HARMONIC @ 2000 RPM
2 ND HARMONIC @ 2000 RPM
3 RD HARMONIC @ 2000 RPM

FIGURE C-10

accurate model propellers made from a type of epoxy glue. The modulus of elasticity, density and strength all appear to have great promise in model propeller applications, since they permit more accurate scaling of the model. The material is light enough in water to have practically no inertial effects of its own. Any inertia of the propeller would be due to the entrained water.

Thus a dramatic reduction in J_p should raise the natural frequency of this mode of vibration to a value high enough to permit system operation at a comfortable ω/ω_n ratio.

Two other frequencies, both concerning the sensor shaft, occur in the middle of the range of interest. Since they result from the construction of the sensor shaft, it is not possible to change these frequencies without starting over from scratch. It is always a possibility that these two frequencies will not occur, so nothing should be done until the system is constructed and in operation.

APPENDIX D - TORSIONAL VIBRATION ANALYSIS COMPUTER PROGRAM

Introduction.

Using the Holzer method of torsional shaft analysis, this IBM 1100 compatible FORTRAN IV program can analyze a shafting system of up to twenty sections for natural frequencies in torsional modes of vibration. The program is written in general terms, using five letter variable names and restricted FORTRAN IV so as to be compatible with the IBM 1100 computer. Easy adaption to other batch processing computer systems is provided by the use of integer variables for I/O statements.

The Holzer method is based on the principle of conservation of energy. In a frictionless system vibrating at its natural frequency, the sum of the potential and kinetic energies will always be a constant. The total maximum potential energy will be equal to the total maximum kinetic energy when the system is vibrating at a natural frequency.

The Holzer method computes kinetic and potential energies for individual components of the system and computes a sum of the two, called remainder torque. When both positive and negative energy contributions from all of the components have been considered and the remainder torque is zero, the system is known to be vibrating at a natural frequency. If the remainder torque is not zero, it means the system is not vibrating in a natural mode and that energy from an external source must be supplied to

force such an unnatural vibration mode.

Input Variables.

Inputs are given names suggestive of the values represented. In order of input into the program, they are:

M — The number of shaft sections in the shaft being analyzed. This is the first value read by the program and is read in I10 format. A maximum of twenty sections may be entered.

DIN(I)
DOUT(I)
LENTH(I) — These are the inner diameter, outer diameter and length dimensions of the shaft section referred to by the program variable "I". Each input card pertains to a separate section of the shaft. DIN(I) may be entered as zero (left blank) to represent a solid shaft section. Dimensions in inches and decimal fractions are assumed. There must be one card for each section, i.e. there should be M cards. The format is 3F10.4

OMEGA
DIVID
NTIME — The assumed starting frequency is OMEGA, in radians per second. The program uses the factor DIVID to compute an increment of change to OMEGA for a series of shaft analyses with different frequencies. NTIME is the number of times that the frequency will be varied

and computations repeated. NTIME may be any integer value. Enter in format E10.4, F10.2, I10.

G(I) G(I) stands for the shear modulus. This quantity is used to compute the shaft stiffness for each assection. The format is 6E12.5 and there must be M values of G supplied.

WEIGT(I) WEIGH is the value of the density for each section in lbs/inch^3. There must be M values supplied to the program in format 6F10.4

PROPI PROPI is the assumed value of propeller inertia. It is treated as an inertia attached to the end of the shaft, and is entered in F10.5 format.

This concludes the definition of all of the input values to the program. Other variables appearing in the program will now be defined.

Program Variables.

SFTIN(I) SFTIN is the computed value of shaft inertia. The rotational inertia of each shaft section is computed and divided by two. One half of the inertia for each section is assumed to be concentrated at the respective ends of the

shaft section. Section inertias from adjacent sections are added and assumed to be inertial disks separated by the length of the shaft.

SFTST(I) — SFTST is the computed value of shaft stiffness between the inertial disks. Units are radians per inch-lb.

RTORQ(I) — RTORQ is the remainder torque. It is the estimated torque in the shaft at the location of the inertial disks.

TORQ(I) — TORQ is the amount of torque required to cause an inertial disk to vibrate with a deflection BETA.

BETA(I) — BETA(I) is the total angle of twist in the shaft at inertial mass I. BETA(I) is assumed equal to 1.0 radians to start the shaft deflection analysis.

PHI(I) — PHI is the angle of twist between two inertial masses. The relationship BETA(I+1) = BETA(I)-PHI(I) is used to iteratively compute BETA.

Program Operating Instructions.

Program inputs must be entered in the order listed

in the section titled "Input Variables" and using the formats specified there. In case format specifications call for more input data than are required by the number of shaft sections, the extra data may be entered as blanks. For example, if there are four sections in the shaft being analyzed, several specifications are 6Fxx.x or 6Exx.x. Enter the first four program constants as indicated and leave the rest of the card blank.

The program makes provisions for computing several sets of data with only one run. A data deck for each shaft si made up in the order listed. A collection of decks for several shafts may be inserted together and as one large deck. A blank card must be placed behind the last shaft description to cause normal program termination.

Interpretation of Output.

The program will give two categories of output data. The first collection of output is a listing of input data with a computed rotational inertia and shaft stiffness for each section. The assumed propeller inertia and the starting frequency are also listed.

The second collection of output is the results of the shaft analysis. There are five columns of output. The first column lists the inertial mass, the second column lists the angular deflection of each mass at the assumed frequency of vibration, the third column gives the torque necessary to cause the respective angular deflections. The fourth column lists the total torque in the shaft at the

inertial mass and the fifth column lists the change in shaft angle of twist between respective inertial masses. The frequency used in computing the columns of data is printed after all of the shaft section data are printed.

The program does not iterate to determine an exact natural frequency, but instead depends upon the user to interpret the results and by successive runs to isolate the natural frequencies. A natural frequency may be detected by noticing a sign shaft in the "Remainder Torque" output data column. If the remainder torque is zero for the last inertial mass, the natural frequency has been determined. Thus during a series of analyses over a range of frequencies, if the sign of the remainder torque for the last shaft element shifts from positive to negative or vice versa, a zero point has been passed and the natural frequency lies between the frequencies of the two successive computations.

Values of BETA may be plotted versus corresponding values of OMEGA to describe the angular deflection of the shaft as a function of operating frequency.

See figure D-1 for a listing of a sample data deck. Pages D-8 through D-10 are a program listing and pages D-11 through D- are sample output results.

Card 1 - Number of shaft sections I10

Card 2 - Dimensions of section (one for each section), 3F10.4

Card 3 - Starting frequency, dividing factor and number of repeats, E10.4, F10.2, I10

Card 4 - Shear modulus for each section - 6E12.5

Card 5 - Density for each section - 6F10.4

Card 6 - Assumed propeller inertia

Card 7 - Blank card to signify end of data to program
Do not insert blank between sets of data.

DATA DECK INSTRUCTIONS

FIGURE D-1

```
      NR=5
      NP=6
      REAL LENTH(20)
      DIMENSION SFTST(20),SFTIN(21), WEIGT(20),DOUT(20),DIN(20),TORQ(20)
      DIMENSION G(20)
      DIMENSION BETA(20),PHI(20)
C   M=NUMBER OF SHAFT SECTIONS
C    A BLANK CARD WILL SET M = ZERO AND WILL CAUSE NORMAL PROGRAM
C    TERMINATION
   21 READ(NR,100)  M
      IF(M-1) 20,1,1
    1 READ(NR,101)(DIN(I),DOUT(I), LENTH(I), I=1,M)
C    OMEGA = ASSUMED STARTING FREQUENCY FOR COMPUTATION
C    DIVID = DIVIDING FACTOR FOR COMPUTING INCREMENTAL CHANGE TO
C    OMEGA FOR ITERATIONS ON FREQUENCY
C    NTIME = NUMBER OF TIMES ITERATIONS ARE PERFORMED
      READ(NR,102) OMEGA, DIVID, NTIME
      READ(NR,103) (G(I), I=1,M)
      READ(NR,104)(WEIGT(I), I=1,M)
      READ(NR,105) PROPI
      PICON=3.141596/32.
C    COMPUTE SHAFT STIFFNESS AND SHAFT SECTION INERTIAS
      DO 10 I=1,M
      CONS1=DOUT(I)*DOUT(I)-DIN(I)*DIN(I)
      CONST=DOUT(I)**4-DIN(I)**4
      SFTST(I)=PICON*CONST*G(I)/LENTH(I)
   10 SFTIN(I)=CONS1*CONS1*LENTH(I)*WEIGT(I)/386.24*PICON
      WRITE(NP,199)
      WRITE(NP,200)  (I,SFTIN(I),DIN(I),DOUT(I),LENTH(I),
     1SFTST(I),WEIGT(I),G(I), I=1,M)
      WRITE(NP,205) PROPI
      WRITE(NP,201) OMEGA
C    COMPUTE OMEG1, THE INCREMENT OF CHANGE OF FREQUENCY
      OMEG1=OMEGA/DIVID
      WRITE(NP,202)
      J=M+1
```

```
C    BEGINNING OF HOLZER ANALYSIS FOR NEW FREQUENCY
       DO 13 L=1,NTIME
       SQOMG=OMEGA*OMEGA
       SMASS=SFTIN(1)
       RTORQ=0.0
      'BETA(1)=1.0
C    BEGIN SHAFT ANALYSIS
       DO 11 I=1,J
       TORQ(I)=SMASS*SQOMG*BETA(I)
       RTORQ=RTORQ+TORQ(I)
       IF(M-I) 16,14,12
    14 SMASS=SFTIN(I)/2.+ PROPI
       GO TO 15
    12 SMASS=(SFTIN(I)+SFTIN(I+1))/2.
       GO TO 15
    15 PHI(I)=RTORQ/SFTST(I)
       BETA(I+1)=BETA(I)-PHI(I)
       WRITE(NP,203) I,BETA(I),TORQ(I),RTORQ,PHI(I)
    11 CONTINUE
    16 PHI(I)=0.0
       WRITE(NP,203) I,BETA(I),TORQ(I),RTORQ,PHI(I)
       WRITE(NP,204)OMEGA
       OMEGA=OMEGA-OMEG1
    13 CONTINUE
   100 FORMAT(I10)
   101 FORMAT(3F10.4)
   102 FORMAT(E10.4,F10.2,I10)
   103 FORMAT(6E12.5)
   104 FORMAT(6F10.4)
   105 FORMAT(F10.5)
   199 FORMAT(1H1,37X,'INPUT QUANTITIES',//,7X,'INERTIA',7X,'DIAMETER',
      1 12X,'LENGTH',5X,'STIFFNESS',5X,'DENSITY',6X,'SHEAR',/,
      2 5X,'IN-LB-SEC**2',4X,'IN',6X,'OUT',9X,'INCHES',5X,'RAD/INCH',
      3 6X,'LB/IN**3',5X,'MODULUS',//)
   200 FORMAT(2X,I2,3X,E10.4,2X,F7.3,2X,F7.3,5X,F7.3,5X,E10.4,4X,F7.3,4X,
      1 E10.4,/)
```

```
201 FORMAT(1H ,///,5X,'INPUT FREQUENCY='E10.4,' RADIANS/SECOND')
202 FORMAT(1H1,37X,'OUTPUT DATA',////,6X,'INERTIA',5X,'BETA',8X,'TORQU
   1E',7X,'REMAINDER',8X,'SHAFT',/,7X,'MASS',5X,'(RADIANS)',3X,'(INCH-
   2LBS)',6X,'TORQUE',7X,'TWIST ANGLE',//)
203 FORMAT(8X,I2,5X,E10.4,4X,E10.4,4X,E10.4,4X,E10.4)
204 FORMAT(1HO,'THE FREQUENCY USED FOR THIS ITERATION WAS ',E10.4,///)
205 FORMAT(2X,'ASSUMED PROPELLER INERTIA=',E10.4)
    GO TO 21
 20 STOP
    END
       4
  1.451    3.400     13.125
.875       2.065     3.435
 .500      2.065     4.535
 .500    1.5000      2.740
.600E 04       120.          20
.11500E 08  .11500E 08  .11500E 08  .11500E 08
   .2860   .2860     .2860      .2860
.0707
       4
  1.451    3.400     13.125
.875       2.065     3.4
 .500      2.065     4.535
 .500    1.5000      2.740
.600E 04       120.          20
.11500E 08  .11500E 08  .11500E 08  .11500E 08
   .2860   .2860     .2860      .2860
.0500
       4
  1.451    3.400     13.125
.875       2.065     3.4
 .500      2.065     4.535
 .500    1.5000      2.740
.600E 04     80.           20
.11500E 08  .11500E 08  .11500E 08  .11500E 08
   .2860   .2860     .2860      .2860
```

	INERTIA IN-LB-SEC**2	DIAMETER IN	OUT	LENGTH INCHES	STIFFNESS RAD/INCH	DENSITY LB/IN**3	SHEAR MODULUS
1	0.8529E-01	1.451	3.400	13.125	0.1111E 08	0.286	0.1150E 08
2	0.3025E-02	0.875	2.065	3.400	0.5843E 07	0.286	0.1150E 08
3	0.5312E-02	0.500	2.065	4.535	0.4511E 07	0.286	0.1150E 08
4	0.7967E-03	0.500	1.500	2.740	0.2060E 07	0.286	0.1150E 08

ASSUMED PROPELLER INERTIA=0.5000E-01

INPUT FREQUENCY=0.6000E 04 RADIANS/SECOND

OUTPUT DATA

INERTIA MASS	BETA (RADIANS)	TORQUE (INCH-LBS)	REMAINDER TORQUE	SHAFT TWIST ANGLE
1	0.1000E 01	0.3070E 07	0.3070E 07	0.2763E 00
2	0.7237E 00	0.1150E 07	0.4221E 07	0.7223E 00
3	0.1399E-02	0.2099E 03	0.4221E 07	0.9357E 00
4	-.9343E 00	-.1027E 06	0.4118E 07	0.1999E 01
5	-.2933E 01	-.5322E 07	-.1204E 07	0.0

FREQUENCY USED FOR THIS ITERATION WAS 0.6000E 04

1	0.1000E 01	0.3019E 07	0.3019E 07	0.2717E 00
2	0.7283E 00	0.1139E 07	0.4158E 07	0.7116E 00
3	0.1675E-01	0.2472E 04	0.4160E 07	0.9222E 00
4	-.9055E 00	-.9792E 05	0.4063E 07	0.1972E 01
5	-.2877E 01	-.5134E 07	-.1071E 07	0.0

FREQUENCY USED FOR THIS ITERATION WAS 0.5950E 04

1	0.1000E 01	0.2969E 07	0.2969E 07	0.2671E 00
2	0.7329E 00	0.1126E 07	0.4095E 07	0.7009E 00
3	0.3201E-01	0.4645E 04	0.4100E 07	0.9088E 00
4	-.8768E 00	-.9323E 05	0.4007E 07	0.1945E 01
5	-.2822E 01	-.4950E 07	-.9434E 06	0.0

FREQUENCY USED FOR THIS ITERATION WAS 0.5900E 04

1	0.1000E 01	0.2919E 07	0.2919E 07	0.2626E 00
2	0.7374E 00	0.1114E 07	0.4033E 07	0.6902E 00
3	0.4718E-01	0.6731E 04	0.4040E 07	0.8955E 00
4	-.8483E 00	-.8868E 05	0.3951E 07	0.1918E 01
5	-.2766E 01	-.4771E 07	-.8197E 06	0.0

FREQUENCY USED FOR THIS ITERATION WAS 0.5850E 04

1	0.1000E 01	0.2869E 07	0.2869E 07	0.2582E 00
2	0.7418E 00	0.1102E 07	0.3971E 07	0.6796E 00
3	0.6226E-01	0.8731E 04	0.3980E 07	0.8822E 00
4	-.8199E 00	-.8425E 05	0.3896E 07	0.1891E 01
5	-.2711E 01	-.4596E 07	-.7003E 06	0.0

FREQUENCY USED FOR THIS ITERATION WAS 0.5800E 04

1	0.1000E 01	0.2820E 07	0.2820E 07	0.2537E 00
2	0.7463E 00	0.1090E 07	0.3909E 07	0.6690E 00

3	0.7725E-01	0.1065E 05	0.3920E 07	0.8689E 00
4	-.7917E 00	-.7995E 05	0.3840E 07	0.1864E 01
5	-.2656E 01	-.4425E 07	-.5849E 06	0.0

FREQUENCY USED FOR THIS ITERATION WAS 0.5750E 04

1	0.1000E 01	0.2771E 07	0.2771E 07	0.2493E 00
2	0.7507E 00	0.1077E 07	0.3848E 07	0.6585E 00
3	0.9215E-01	0.1248E 05	0.3860E 07	0.8557E 00
4	-.7636E 00	-.7578E 05	0.3785E 07	0.1837E 01
5	-.2601E 01	-.4258E 07	-.4736E 06	0.0

FREQUENCY USED FOR THIS ITERATION WAS 0.5700E 04

1	0.1000E 01	0.2723E 07	0.2723E 07	0.2450E 00
2	0.7550E 00	0.1064E 07	0.3787E 07	0.6481E 00
3	0.1070E 00	0.1423E 05	0.3801E 07	0.8426E 00
4	-.7356E 00	-.7173E 05	0.3729E 07	0.1810E 01
5	-.2546E 01	-.4096E 07	-.3664E 06	0.0

FREQUENCY USED FOR THIS ITERATION WAS 0.5650E 04

1	0.1000E 01	0.2675E 07	0.2675E 07	0.2407E 00
2	0.7593E 00	0.1052E 07	0.3726E 07	0.6377E 00
3	0.1217E 00	0.1591E 05	0.3742E 07	0.8295E 00
4	-.7078E 00	-.6780E 05	0.3674E 07	0.1783E 01
5	-.2491E 01	-.3937E 07	-.2631E 06	0.0

FREQUENCY USED FOR THIS ITERATION WAS 0.5600E 04

1	0.1000E 01	0.2627E 07	0.2627E 07	0.2364E 00
2	0.7636E 00	0.1039E 07	0.3666E 07	0.6273E 00
3	0.1363E 00	0.1750E 05	0.3683E 07	0.8164E 00
4	-.6802E 00	-.6399E 05	0.3619E 07	0.1757E 01
5	-.2437E 01	-.3783E 07	-.1637E 06	0.0

FREQUENCY USED FOR THIS ITERATION WAS 0.5550E 04

1	0.1000E 01	0.2580E 07	0.2580E 07	0.2321E 00
2	0.7679E 00	0.1026E 07	0.3606E 07	0.6170E 00
3	0.1508E 00	0.1902E 05	0.3625E 07	0.8035E 00
4	-.6527E 00	-.6031E 05	0.3564E 07	0.1730E 01
5	-.2383E 01	-.3633E 07	-.6821E 05	0.0

FREQUENCY USED FOR THIS ITERATION WAS 0.5500E 04

1	0.1000E 01	0.2533E 07	0.2533E 07	0.2279E 00
2	0.7721E 00	0.1013E 07	0.3546E 07	0.6068E 00

3	0.1652E 00	0.2046E 05	0.3566E 07	0.7905E 00
4	-.6253E 00	-.5673E 05	0.3510E 07	0.1704E 01
5	-.2329E 01	-.3486E 07	0.2351E 05	0.0

FREQUENCY USED FOR THIS ITERATION WAS 0.5450E 04

1	0.1000E 01	0.2487E 07	0.2487E 07	0.2238E 00
2	0.7762E 00	0.9995E 06	0.3487E 07	0.5967E 00
3	0.1796E 00	0.2183E 05	0.3508E 07	0.7777E 00
4	-.5981E 00	-.5327E 05	0.3455E 07	0.1677E 01
5	-.2275E 01	-.3344E 07	0.1115E 06	0.0

FREQUENCY USED FOR THIS ITERATION WAS 0.5400E 04

1	0.1000E 01	0.2441E 07	0.2441E 07	0.2197E 00
2	0.7803E 00	0.9863E 06	0.3427E 07	0.5865E 00
3	0.1938E 00	0.2312E 05	0.3451E 07	0.7649E 00
4	-.5711E 00	-.4993E 05	0.3401E 07	0.1651E 01
5	-.2222E 01	-.3205E 07	0.1958E 06	0.0

FREQUENCY USED FOR THIS ITERATION WAS 0.5350E 04

1	0.1000E 01	0.2396E 07	0.2396E 07	0.2156E 00
2	0.7844E 00	0.9730E 06	0.3369E 07	0.5765E 00
3	0.2079E 00	0.2435E 05	0.3393E 07	0.7521E 00
4	-.5442E 00	-.4669E 05	0.3346E 07	0.1624E 01
5	-.2168E 01	-.3070E 07	0.2765E 06	0.0

FREQUENCY USED FOR THIS ITERATION WAS 0.5300E 04

1	0.1000E 01	0.2351E 07	0.2351E 07	0.2115E 00
2	0.7885E 00	0.9596E 06	0.3310E 07	0.5665E 00
3	0.2220E 00	0.2550E 05	0.3336E 07	0.7395E 00
4	-.5175E 00	-.4357E 05	0.3292E 07	0.1598E 01
5	-.2116E 01	-.2939E 07	0.3537E 06	0.0

FREQUENCY USED FOR THIS ITERATION WAS 0.5250E 04

1	0.1000E 01	0.2306E 07	0.2306E 07	0.2075E 00
2	0.7925E 00	0.9462E 06	0.3252E 07	0.5566E 00
3	0.2359E 00	0.2659E 05	0.3279E 07	0.7268E 00
4	-.4910E 00	-.4055E 05	0.3239E 07	0.1572E 01
5	-.2063E 01	-.2811E 07	0.4273E 06	0.0

FREQUENCY USED FOR THIS ITERATION WAS 0.5200E 04

1	0.1000E 01	0.2262E 07	0.2262E 07	0.2035E 00
2	0.7965E 00	0.9328E 06	0.3195E 07	0.5467E 00

3	0.2497E 00	0.2761E 05	0.3222E 07	0.7143E 00
4	-.4646E 00	-.3764E 05	0.3185E 07	0.1546E 01
5	-.2010E 01	-.2687E 07	0.4975E 06	0.0

FREQUENCY USED FOR THIS ITERATION WAS 0.5150E 04

1	0.1000E 01	0.2218E 07	0.2218E 07	0.1996E 00
2	0.8004E 00	0.9193E 06	0.3138E 07	0.5370E 00
3	0.2634E 00	0.2857E 05	0.3166E 07	0.7018E 00
4	-.4384E 00	-.3483E 05	0.3131E 07	0.1520E 01
5	-.1958E 01	-.2567E 07	0.5643E 06	0.0

FREQUENCY USED FOR THIS ITERATION WAS 0.5100E 04

1	0.1000E 01	0.2175E 07	0.2175E 07	0.1957E 00
2	0.8043E 00	0.9057E 06	0.3081E 07	0.5272E 00
3	0.2771E 00	0.2946E 05	0.3110E 07	0.6894E 00
4	-.4124E 00	-.3212E 05	0.3078E 07	0.1494E 01
5	-.1906E 01	-.2450E 07	0.6278E 06	0.0

FREQUENCY USED FOR THIS ITERATION WAS 0.5050E 04

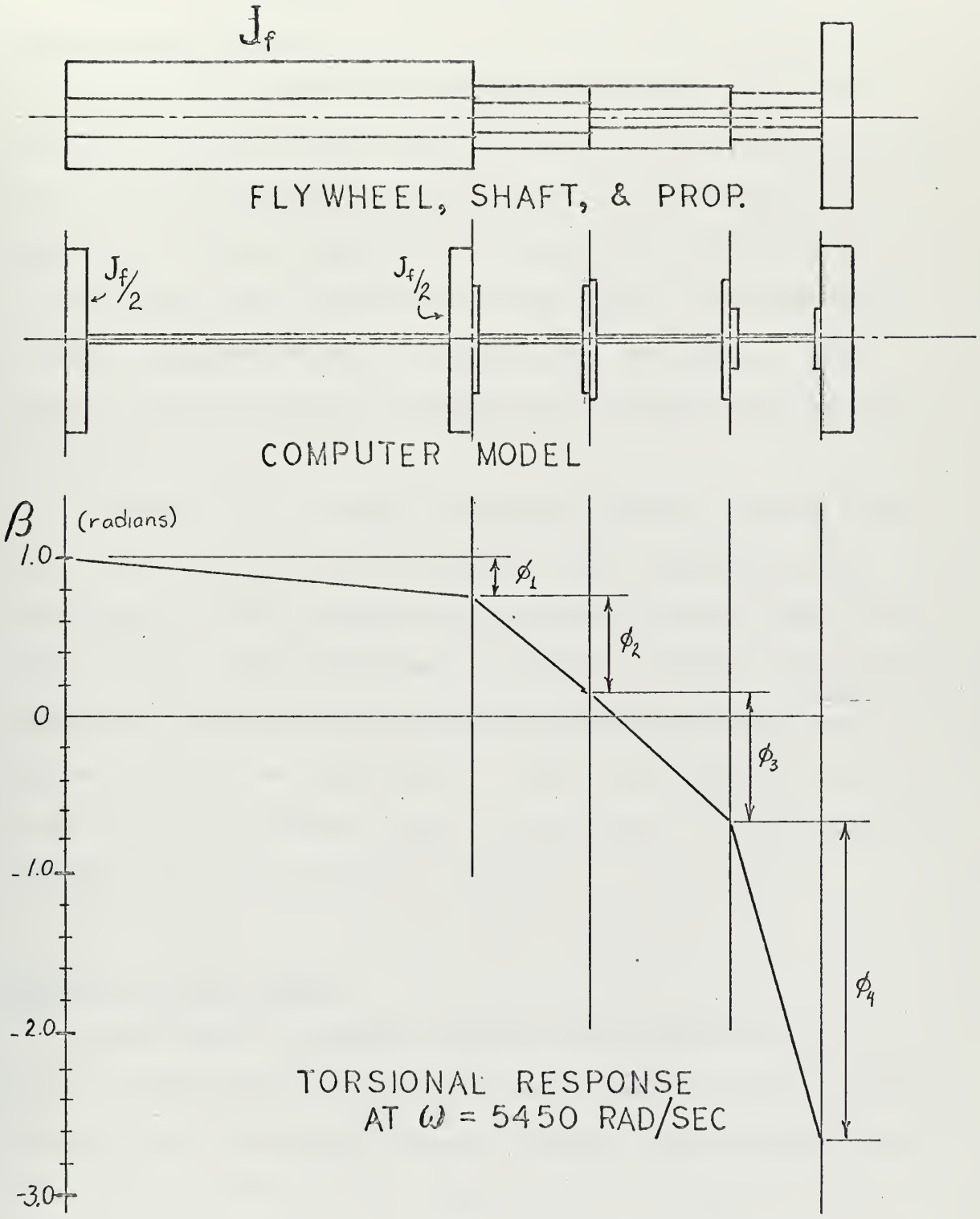

TORSIONAL RESPONSE OF MEASURING UNIT SHAFT NEAR A NATURAL FREQUENCY

FIGURE D-1

APPENDIX E - STRAIN GAGE MOUNTING AND WIRING

Strain Gage Bridges.

Thin wire, foil and semiconductor strain gages all operate on the principle that a change in the length of the gage causes a change in the electrical resistance of the gage. Accordingly, gages are aligned with the direction of principal stress (strain) for the force being measured so that a maximum strain is applied to the gages. Most strain gages are placed in Wheatstone bridges such as the one shown in figure E-2.

A steady D.C. voltage is applied between points A and B of this representative network. When unstressed, the resistances in the network are balanced and the signal voltage is zero. When stressed, the pair of gages in compression has a decrease in resistance and the pair in tension has an increase in resistance. Since these pairs are wired so as to be on opposite legs of the bridge, a difference in voltage appears as an output between points C and D.

Mounting of the Gages.

Gages used to measure torsion are placed at a 45^{o} angle to the axis of the shaft, since that is the direction of principal stress for torsion. Gages which measure axial force are mounted with the long axis of the gages of two opposite legs parallel to the shaft axis and the long axis of the other two opposite legs perpendicular to the shaft axis. This placement takes advantage of both longitudinal

and transverse strains to sense axial forces. Gages are placed in two parallel planes to measure side and vertical forces. Placement in two planes is necessary to cancel effects of shaft bending induced by side forces. Bending moments may be measured by gages in only one plane.

Foil gages, which have a large strain capacity but low output, must be used to measure thrust and torque. Semiconductor gages are appropriate for the other forces and moments because of their higher output and smaller load capacity.

Figure E-1 shows the location of the strain gages on the sensor shaft. Figures E-2 through E-7 show the location of gages in the six bridge networks and the schematic diagram for each. Figure E-8 is a typical schematic diagram for one of the amplifier circuits. All six circuits are similar.

Calibration of the Sensor.

A static calibration of the individual bridge network responses was performed by Mr. Ronald Noret of MIT IL-7 (Draper Laboratory) using a specially constructed mounting to hold the measuring unit shaft [18]. Known pure forces and moments were applied to the sensor by using a bar attached to the propeller mounting taper in conjunction with weights and pulleys. The major effort of this calibration was to determine static output from the six gage bridges, and only a relatively small amount of time was

spent trying to determine crosstalk between bridges. The crosstalk is most important to determine, since this corresponds to the influence coefficients discussed in Appendix A. After the static crosstalk terms are determined, it will be necessary to perform a dynamic calibration as discussed in Appendix A and by Brandau in [19]. A method similar to that used by Brandau is recommended. The use of the special sensor shaft mounting table in conjunction with mechanical shakers described by Brandau should make the dynamic calibration effort relatively straightforward.

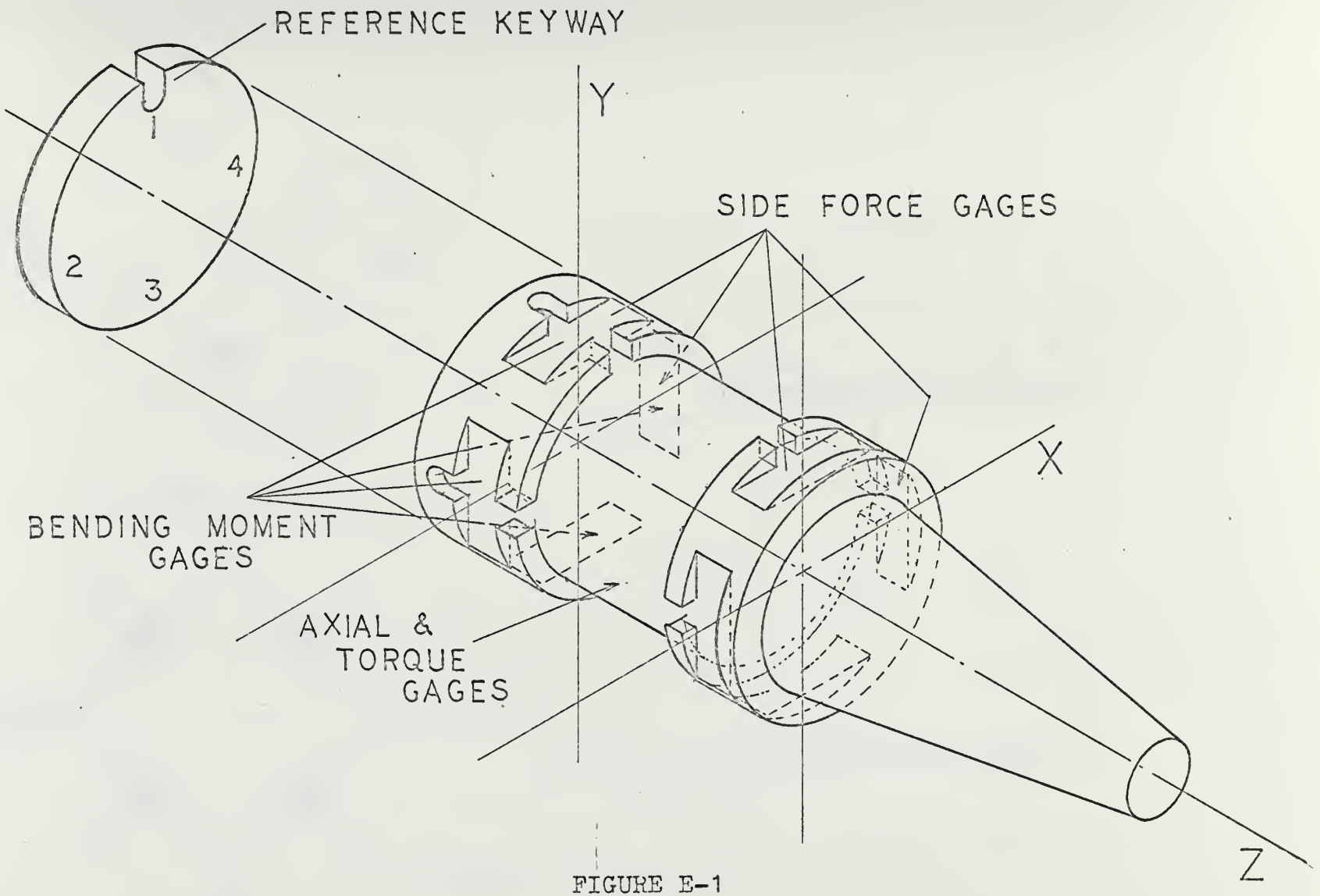
REFERENCE KEYWAY
Y
1
2
3
4
SIDE FORCE GAGES
X
BENDING MOMENT
GAGES
AXIAL &
TORQUE
GAGES
Z

FIGURE E-1

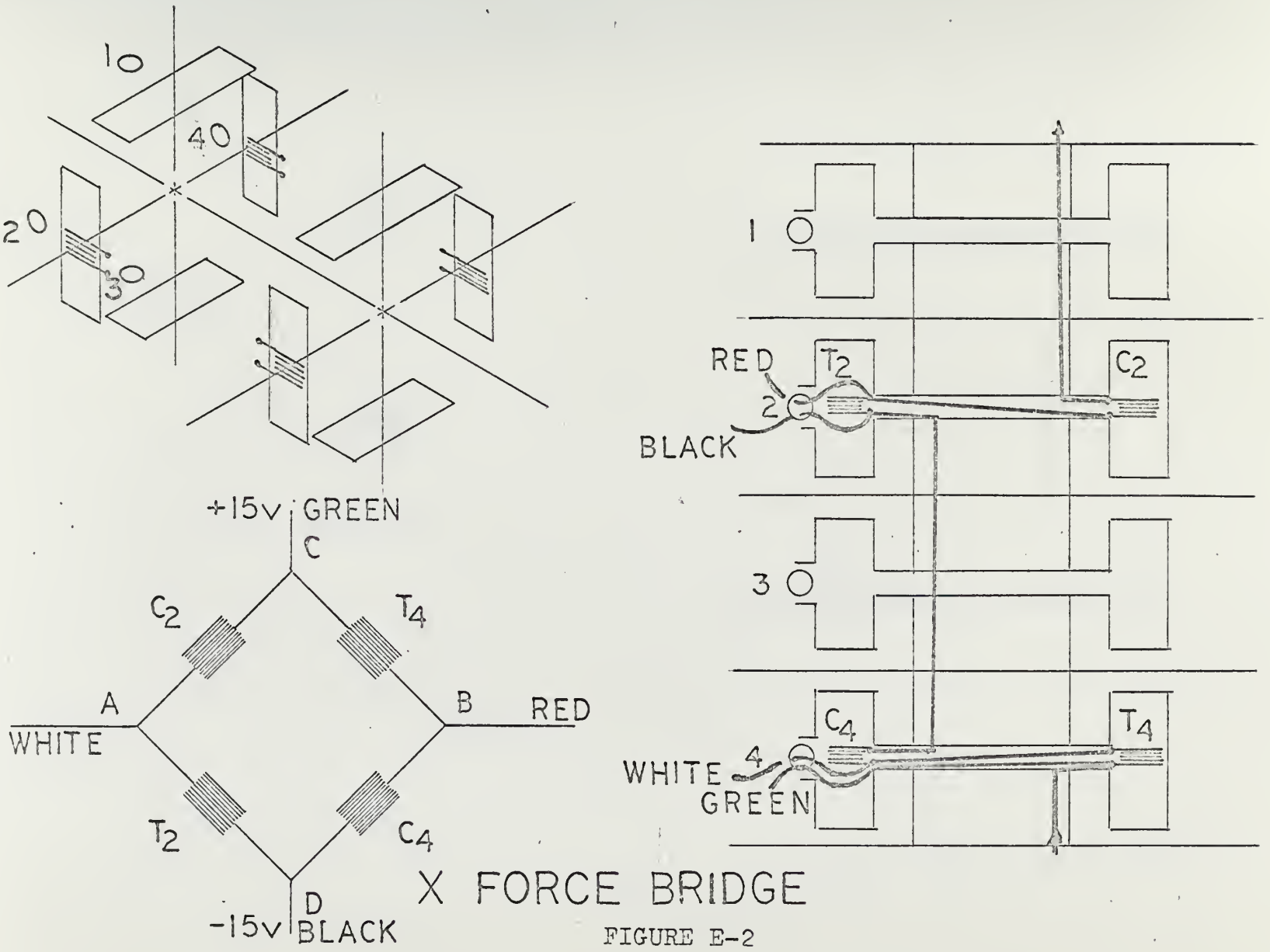

X FORCE BRIDGE

FIGURE E-2

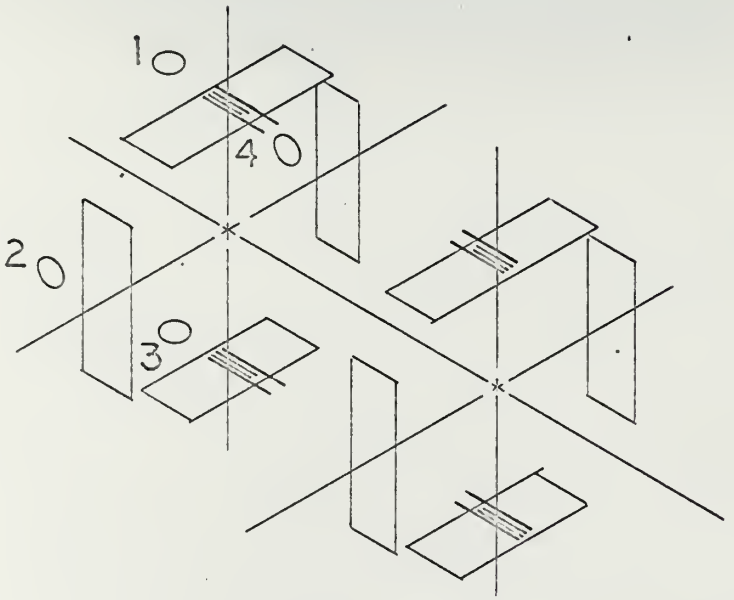

+15v GREEN

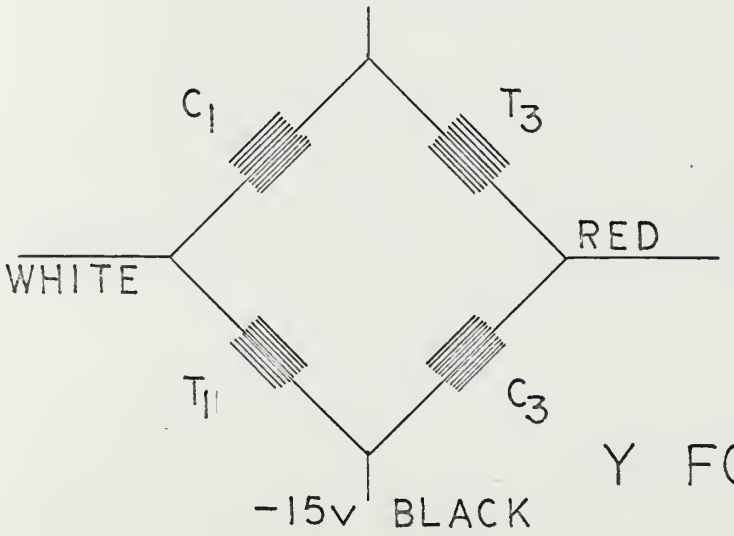

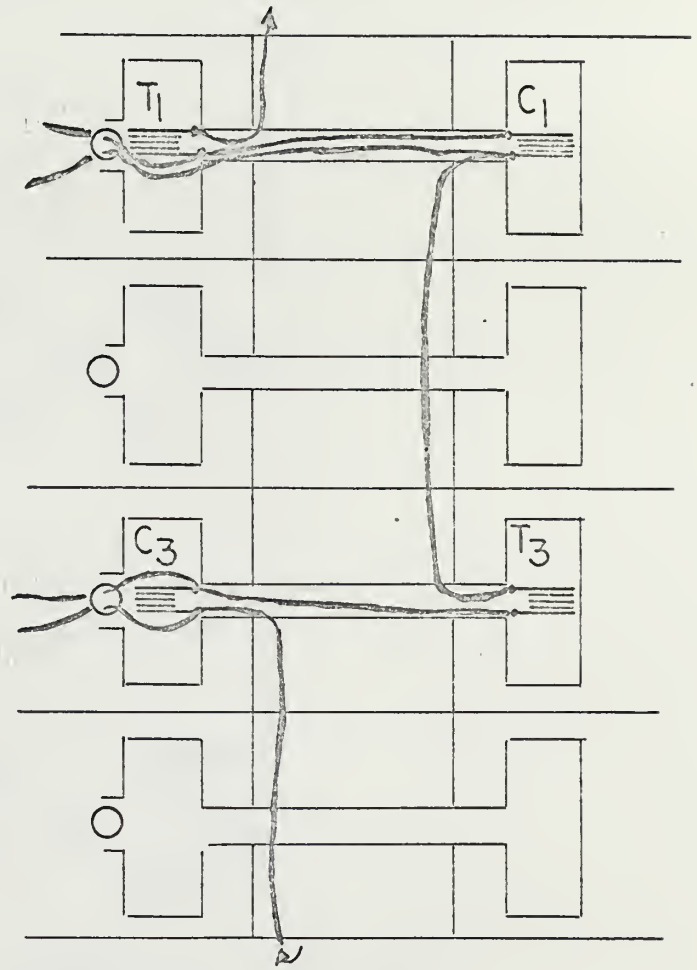

Y FORCE BRIDGE

FIGURE E-3

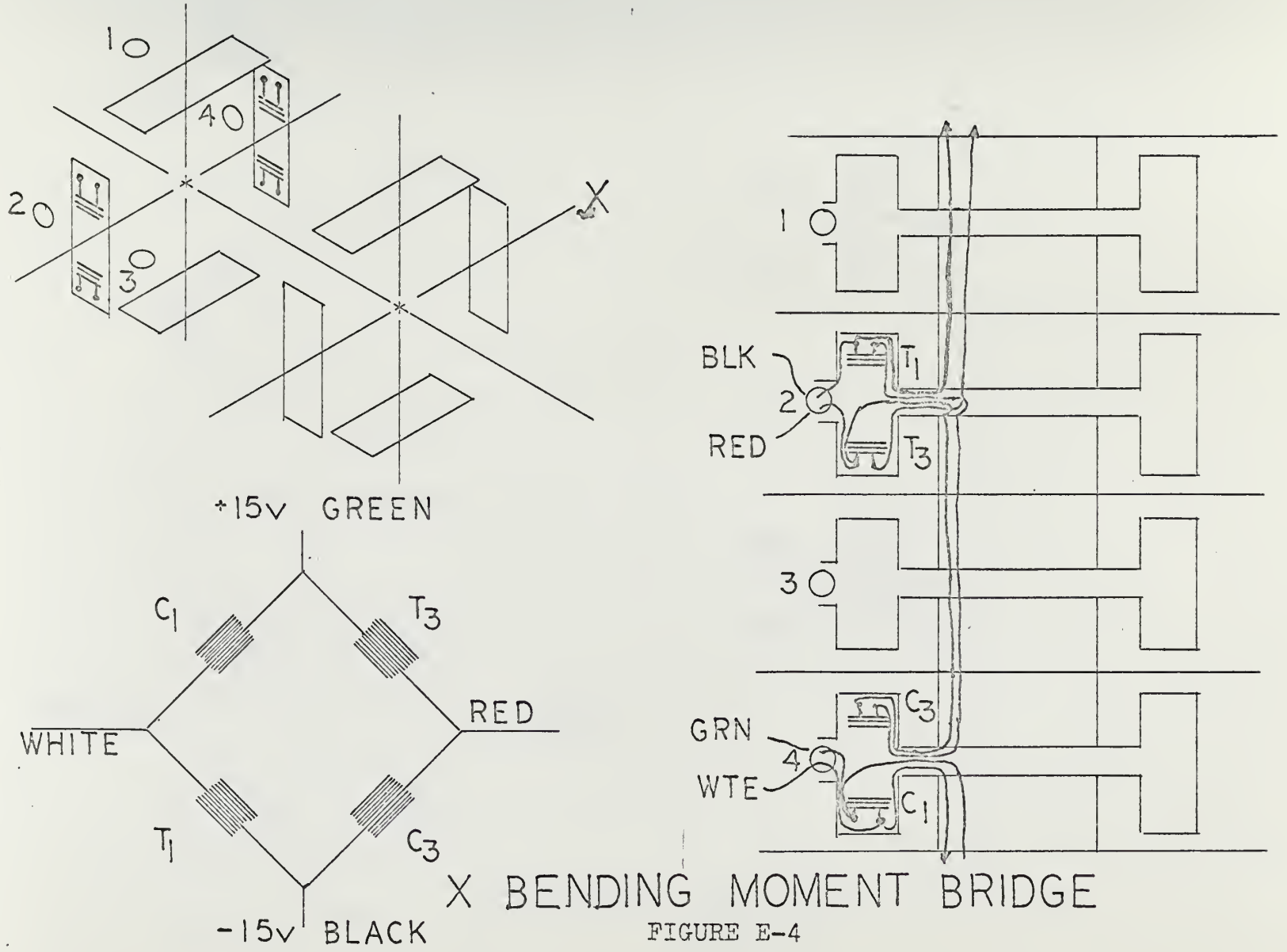

X BENDING MOMENT BRIDGE

FIGURE E-4

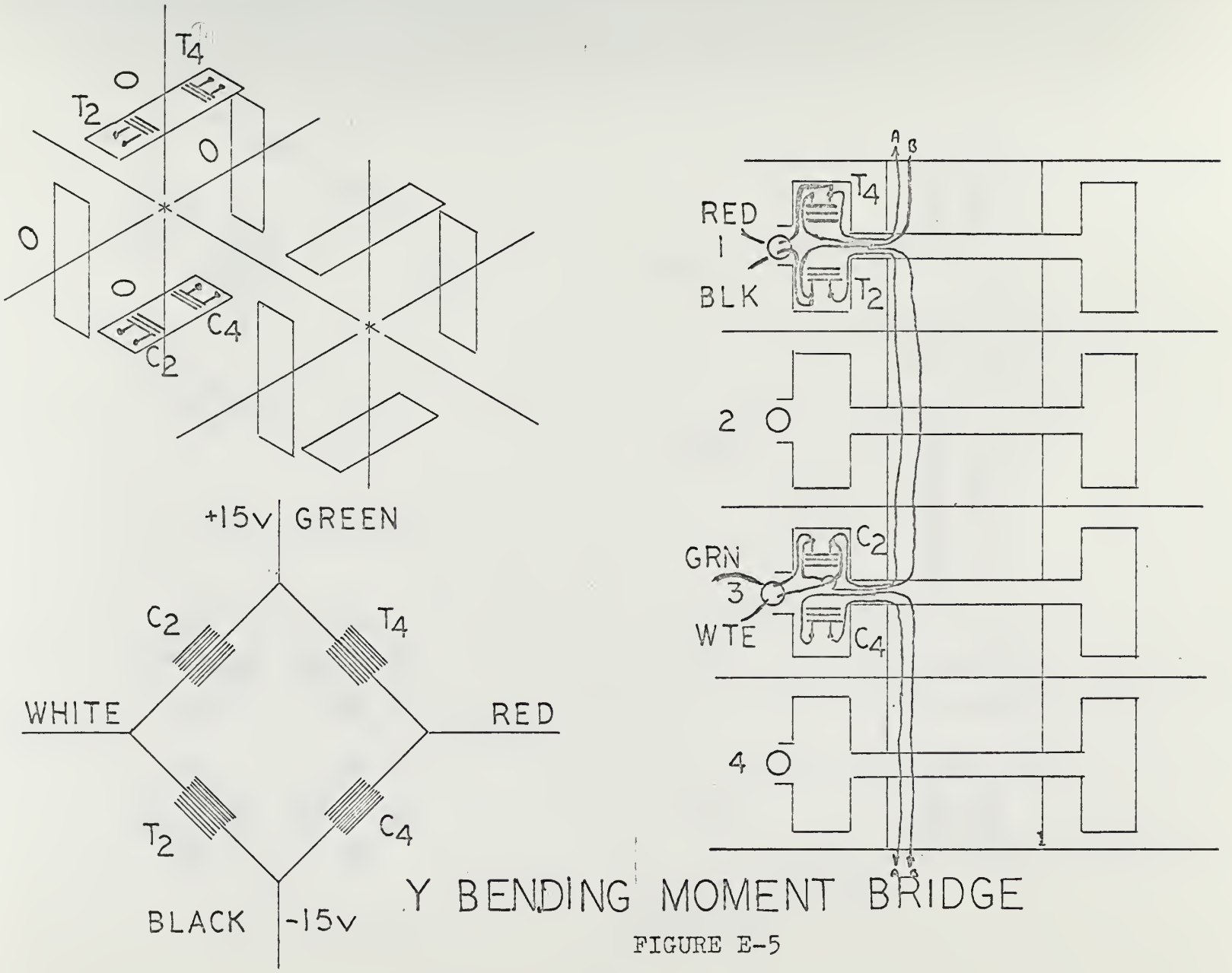

Y BENDING MOMENT BRIDGE

FIGURE E-5

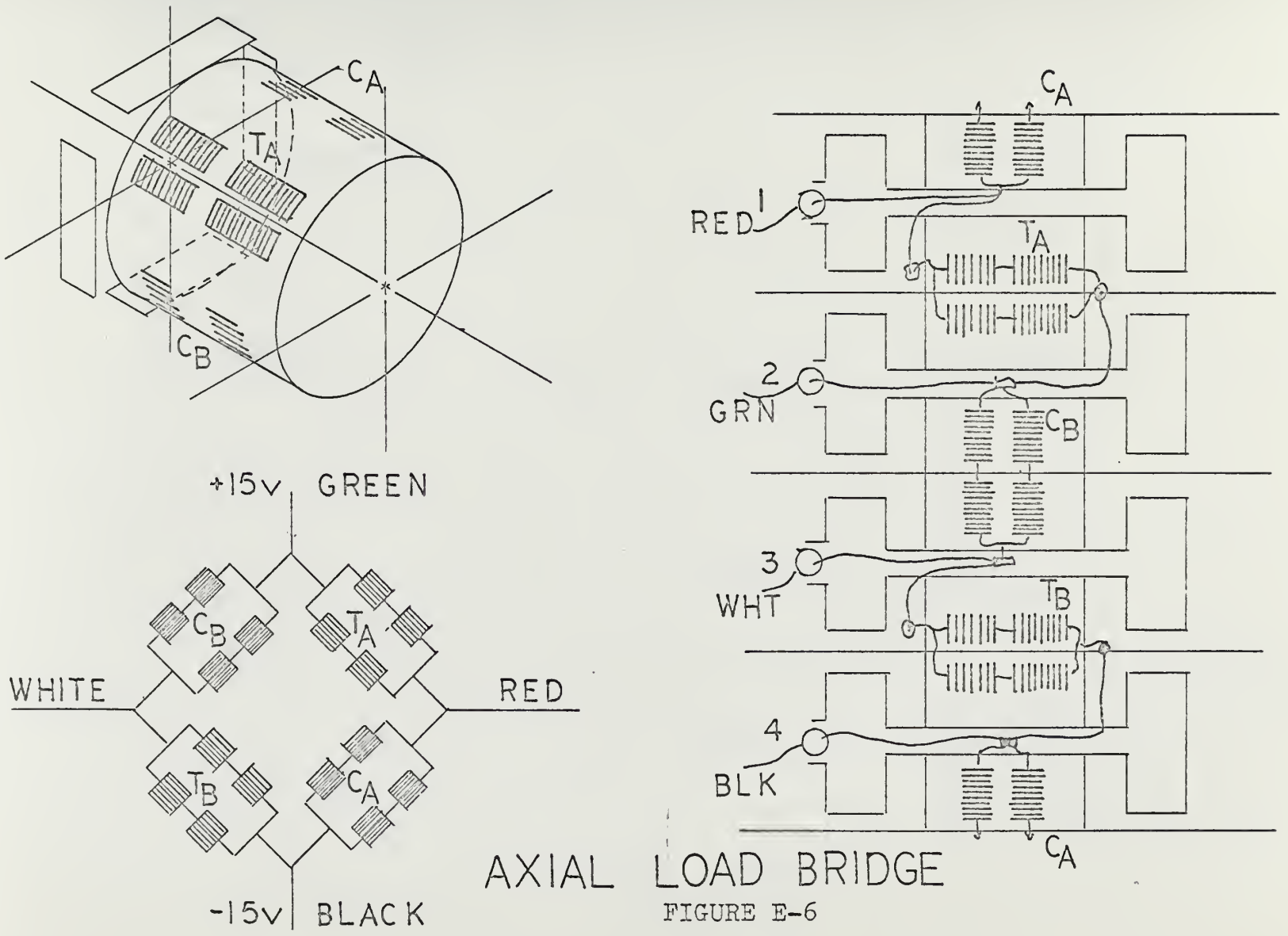

AXIAL LOAD BRIDGE

FIGURE E-6

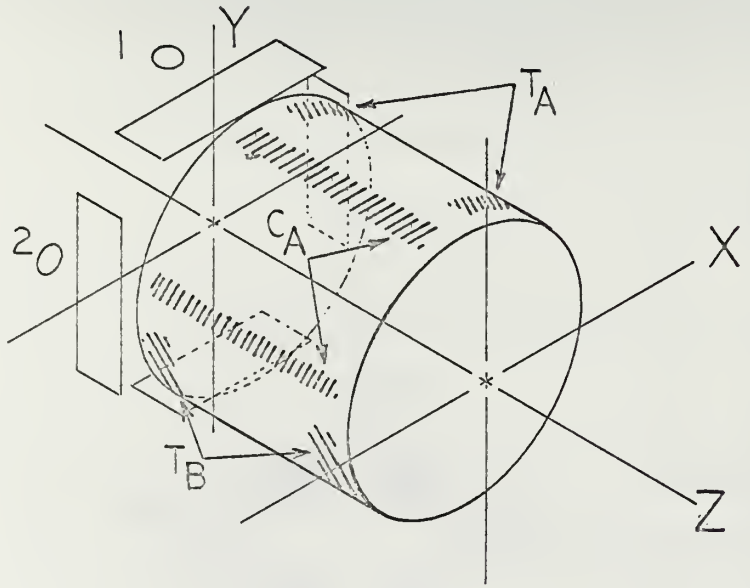

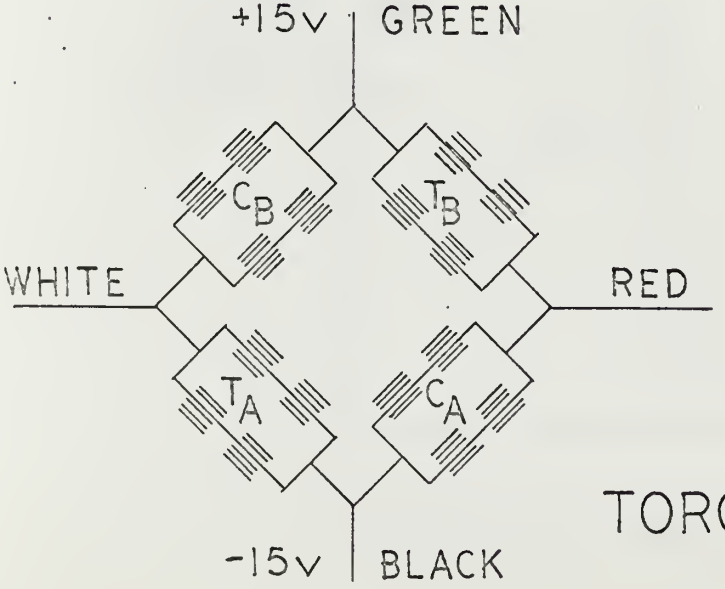

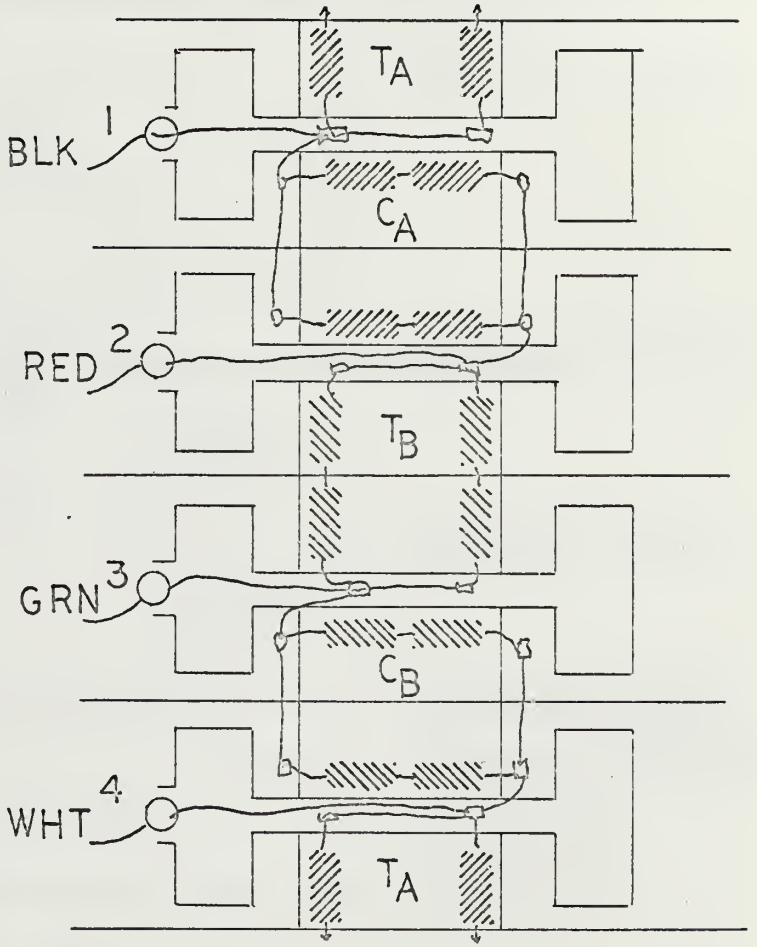

TORQUE BRIDGE

FIGURE E-7

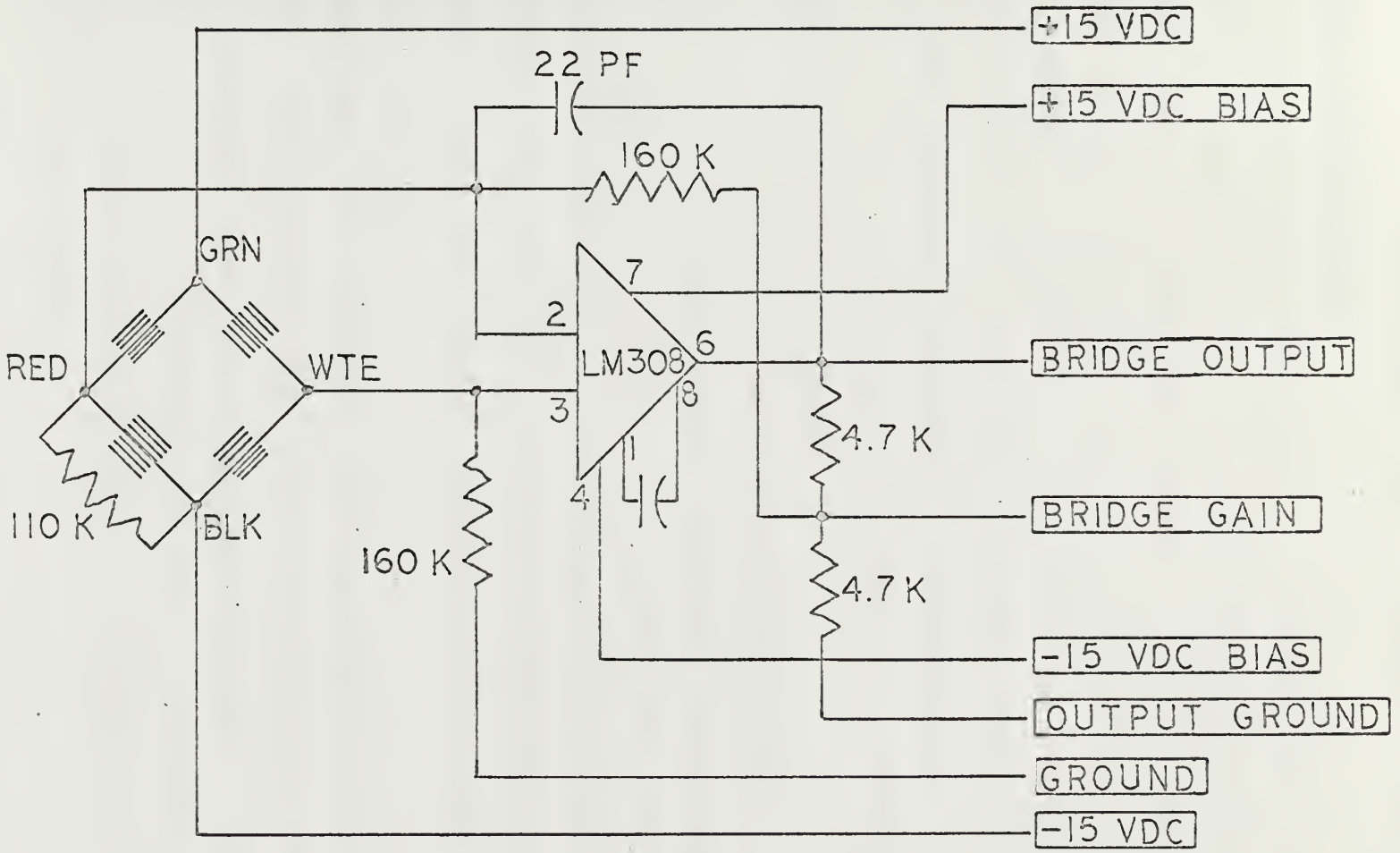

TYPICAL BRIDGE AMPLIFIER CIRCUIT

FIGURE E-8

APPENDIX F - SIX DEGREE OF FREEDOM SENSOR AND PROPELLER SHAFT ASSEMBLY PROCEDURES

General Considerations.

As a starting condition, it is assumed that the two-degree of freedom shaft and all associated parts have been removed from the tunnel and that the tunnel has been drained enough to lower the water level below the test section.

Tables F-1 through F-3 list the major sub-assemblies and component parts. Consider the sensor and shaft system as being composed of three major sub-assemblies.

1. Measuring Unit Assembly (Instrumentation Laboratory Drawing No 167086)
2. Drive Shaft and Housing Assembly
3. Slip Ring and Outer Drive Shaft Assembly

Pieces in the assembly instructions are referred to by name and code number as per appropriate drawings or sketches. The names used in assembly instructions correspond to names given on MIT Instrumentation Lab drawings, as do code numbers.

Precautions All components are finely machined precision parts. Most parts are type 303 or 304 stainless steel and have machined thread fits. Care must be taken to ensure that these parts are properly threaded. A lubricant containing molybdenum disulfide (MS_2) is necessary for joining stainless steel parts.

Special care must be taken to avoid damaging the brass couplings used as drive shaft bearing holders and

connectors between drive shaft housing sections.

Avoid handling metal components except for assembly because most have had passivating surface treatment to inhibit corrosion.

Care must be taken when inserting O-ring seals so that they are not damaged by the sharp edges of threads. Thread damage to O-rings may be prevented by covering the threads with a layer of paper or tape prior to slipping the O-ring into place over the threads.

Some individual parts of the system are quite heavy. Allowing them to hang freely with only the drive shaft or couplings as a support may cause damage to threads or bearings or bend the shaft. Therefore, keep all assembled pieces supported in such fashion that their axes of rotation coincide with the shaft axis of rotation.

The six degree of freedom shaft assembly has been sized to permit complete insertion into the tunnel while fully assembled. All parts are best protected when fully assembled. Therefore, it is recommended that the Measuring Unit Assembly and the Shaft Housing Assembly be put together and joined in one continuous process.

A clean floor space approximately 19 feet long and 6 to 8 feet wide is recommended for an assembly area. The entire shaft assembly will weigh approximately 200 pounds, so several men will be required to lift it and insert it into the tunnel.

TABLE F-1

MEASURING UNIT ASSEMBLY

Ref. No.	Item	Quan.	Material
1	Measuring Element	1	
2	Flywheel	1	
3	Propeller Shaft Adapter	1	
4	Front Housing	1	
5	Intermediate Housing	1	
6	Flywheel Housing	1	
7	Floating Bearing Housing Assembly	1	
8	Timing Unit Assembly	1	
9	Protective Cover (installed on #1)		
10	Screw No. 2-56 UNC-2A Button Head 3/16 Lg self lock	4	SST
11	Screw No. 1/4-20 UNC-2A Soc. Head 1/2 LG Self Lock	12	SST
13	Parker O-Ring 2-044	3	E-540-8
14	Parker O-Ring 2-225	2	E-540-8
15	Rotary Seal, C. E. Conover Rev-O-Slide C53-136	1	N-256-8
16	Rotary Seal, C. E. Conover Rev-O-Slide C53-134	1	N-256-8
17	Bearing, Garlock 32 DU 24	1	
18	Connector, 37 Pin, MD-53	1	
19	Ball (.1247 in. diameter)	4	SST-440C

TABLE F-2

DRIVE SHAFT AND HOUSING ASSEMBLY

Item	Quan.	Material
Drive Shaft	1	SST
Downstream Shaft Housing Section	1	SST
Shaft Housing Section	3	SST
End Housing Section	1	SST
Housing Coupling and Bearing Holder	4	Brass or Bronze
Bearings	8	Mild Steel
O-Ring Seals	9	
Rotary Seal	1	

TABLE F-3

SLIP RING AND OUTER DRIVE SHAFT ASSEMBLY

Item	Quan.	Material
Slip Ring Unit	2	Lebow, Inc
Slip Ring Shaft	1	SST
RPM Signal Pickup and Gear	1	Lebow, Inc
Thrust Bearing	1	
Slip Ring Assembly Housing	1	

Assembly of the Propeller Drive Shaft and Housing.

1. Inspect the drive shaft surface for flaws in the finish. Mark the approximate bearing locations with a soft lead pencil. If low spost appear in the intended bearing locations, swap the shaft end for end.

2. Insert the teflon coated mild steel bearings in all brass shaft housing couplings.

3. Screw one coupling on to the section of the drive shaft housing which mates to the Floating Bearing Housing Assembly [(7) on drawing IL-167086]. Insert an O-ring seal between the housing section and the coupling. (This bearing housing has a special thread on the upstream end. Thus there will be one shaft housing section with different threads on each end. The other three will be interchangable.)

4. Slide this section over the drive shaft into the approximate final position on the drive shaft. Support the housing end which is not attached to a coupling in order to avoid thread damage to either end.

5. Screw the brass couplings on to one end of each of the remaining 36 inch housing sections. Insert O-rings at this time, observing protective precautions.

6. Slide each shaft housing section over the shaft and attach it to the coupling already there. Repeat until all pieces but the end section are installed. Install the remaining O-rings on the couplings at this time. Observe precautions.

At this point, the drive shaft has a protective housing over most of its length. Work under way may be temporarily halted here, or may be continued into the next phase. The next phase should be completed without major interruption.

Assembly of the Measuring Unit Sub-assembly.

The following steps are the recommended order of assembly:

1. Start with the Floating Bearing Housing Assembly (7).

2. Insert the Propeller Shaft Adapter (3) into the Floating Bearing Housing Assembly (7).

3. Attach the Propeller Shaft Adapter (3) to the Propeller Drive Shaft (188 inch long stainless steel tubing with 16 microinch finish).

4. Feed signal leads through the Flywheel (2) and coil around foam rubber piece to act as securing device. A coil similar to that shown on plan 167086 can be achieved by

coiling the signal lead cable about the foam rubber, tensioning the coil to reduce the outer diameter and sliding it into the flywheel. The rubber and coil will then spring back to fill the void areas.

5. Next, feed the signal leads through the Drive Shaft. If the cable is stiff enough, it may be pushed through directly. Otherwise, feed a weighted string through and then pull the signal lead through with the string.

6. Now attach the Flywheel (2) to the Propeller Shaft Adapter (3). To accomplish this, push the Floating Bearing Housing Assembly (7) back on the drive shaft a few inches to gain necessary working clearance to install screws holding the flywheel to the shaft adapter. Install Parker O-ring (14) at this time. During this step, a wooden cradle should be used to support the heavy flywheel in order to avoid crushing the soft support material in the bearing assembly.

7. Install Flywheel Handle (see Figure F-1) on the downstream end of the flywheel. This is to provide a means of supporting the flywheel while performing step 8. The flywheel Handle serves as a dummy Measuring Unit Shaft.

8. Slide the Flywheel Housing (6) over the Flywheel and attach it to the Floating Bearing Housing Assembly (7).

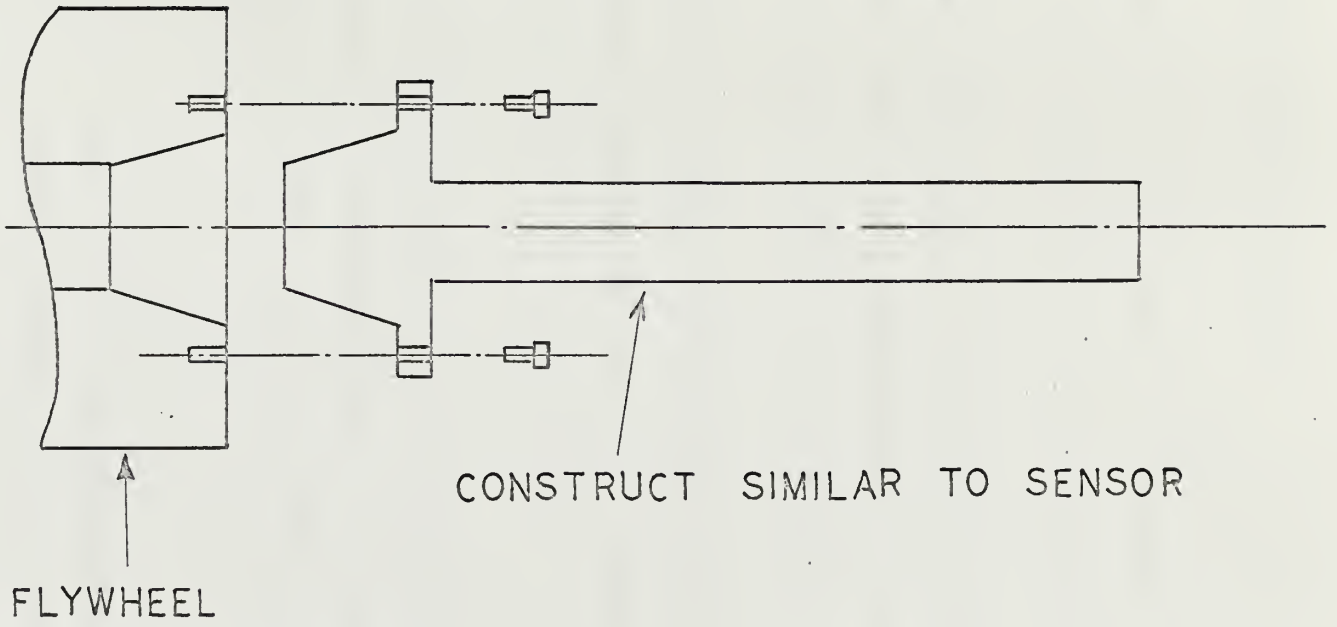

FLYWHEEL HANDLE

FIGURE F-1

Use small wooden wedges, such as tongue depressors as spacers to avoid scarring either the housing or the flywheel or bending the flywheel-shaft adapter connecter.

9. Remove the flywheel handle.

10. Pull the 37 pin connector (18) from the Flywheel and attach it to its mating half in the measuring element (1).

11. Allow the signal cable to spring back into the flywheel and attach the Measuring Element (1) to the Flywheel. Insert Parker O-Ring, 2-225, (14) during this step.

12. Push the drive shaft, flywheel and measuring assembly into the Flywheel Housing (6) until the Timing Unit Assembly (8) is against the Flywheel Housing.

13. Align the ball bearings on the Timing Unit Assembly (6) with the slots in the Flywheel Housing (8) and push the entire shaft approximately $\frac{1}{2}$ inch until the ball bearings rest in the slots.

14. Insert Rotary Seal (15) in the Intermediate Housing (5) and screw the Intermediate Housing and the Front Housing (4) together.

15. Slide the Front and Intermediate Housing over the

Measuring Unit (1), being careful not to damage the rotary seal, and attach them to the Flywheel Housing. Install the Parker O-Ring, 2-044 (13) during this step.

This completes the assembly of the Measuring Unit Subassembly. This subassembly should now be joined to the Drive Shaft and Housing Subassembly.

At this point, only the shaft housing and piece remains to be fitted. The end housing section contains the rotating water seal and may contain the thrust bearing. Since the design of the end housing and the slip ring subassembly was not firm as of this writing, no detailed description of the assembly process for the remainder of the system is possible. Some considerations and recommendations are appropriate, however.

Design Considerations for the Slip Ring Assembly.

A primary constraint exists on the overall length of the Slip Ring Housing and Assembly. The total length of the drive shaft, housings and slip ring assemblies, when joined, must be less than 18½ feet. The maximum length of 18½ feed derives from the clearance between the building wall and the tunnel wall where the drive shaft is to be inserted.

As short a length as is reasonably possible then, is a goal to achieve in the design of the slip ring assembly, since the length of the shaft which fits within the

tunnel is fixed.

Slip rings of Lebow manufacture are recommended. The Model 6116-8 unit is recommended over the Model 6105-8. The units are similar except for price, diameter of the rotating shaft, and length. The Model 6116-8 has 8 slip rings, a length of 4 3/8 inches and accomodates a shaft diameter equal to 1.5 inches. The Model 6105-8 also has 8 slip rings, but is 5.06 inches long and accomodates a shaft diameter of 1.0 inches. However, the Model 6105-8 is $180 cheaper.

Two units with 8 slip rings each are recommended. Fourteen rings are required, but since slip ring sets come in multiples of four, two extra leads are incorporated into the signal cable. Custom order slip ring sets with up to 20 rings are available, but at a premium price.

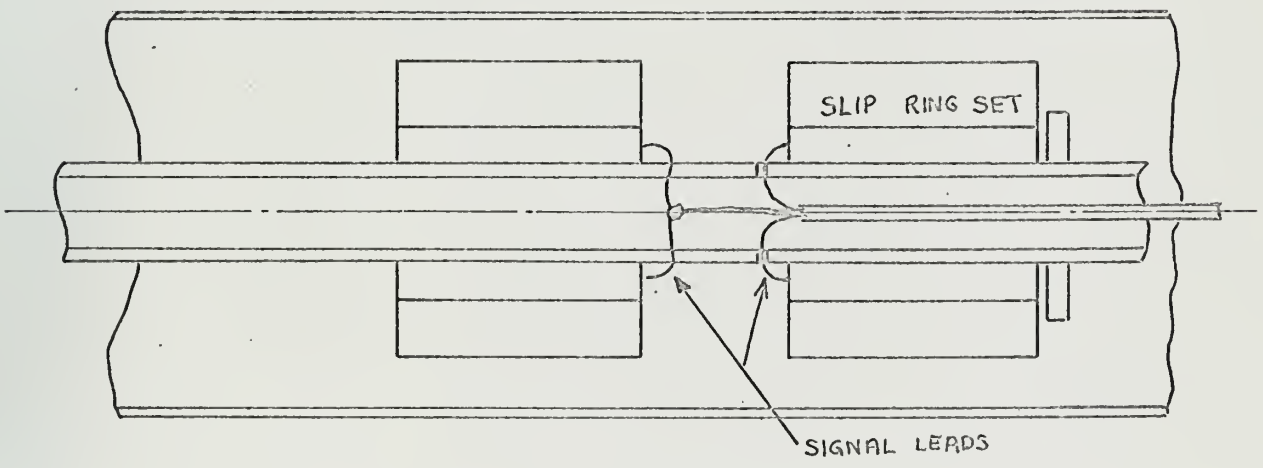

SLIP RING SUB ASSEMBLY

FIGURE F-2

The proposed method of using the slip rings is shown in Figure F-2. Dimensional constraints are that the length L must be less than 22 inches and that the access distance A must be sufficient to solder the signal leads to the slip ring terminal posts. Another important concern is the task of feeding the signal leads through the slip ring shaft and out through the drilled holes. Accomplishing this feat with a small diameter shaft will be difficult at best.

For this reason, as well as the length savings, the Model 6118-8 units are recommended. The extra one-half inch of shaft O.D. will permit a larger shaft I.D. and larger holes through which to feed the cable leads.

Four staggered holes are recommended, two for each slip ring set. Spacing between them should be such that they do not lie on the same 45 degree helical line in order to avoid drilling one hole in the torsion induced stress field of another.

Thesis
H804 Horton
118373
Design and construction of a system for measurement of unsteady propeller forces.